

# DERIVING FINITE SPHERE PACKINGS

NATALIE ARKUS, VINOTHAN N. MANOHARAN AND MICHAEL P. BRENNER

**ABSTRACT.** Sphere packing problems have a rich history in both mathematics and physics; yet, relatively few analytical analyses of sphere packings exist, and answers to seemingly simple questions are unknown. Here, we present an analytical method for deriving all packings of  $n$  spheres in  $\mathbb{R}^3$  satisfying minimal rigidity constraints ( $\geq 3$  contacts per sphere and  $\geq 3n - 6$  total contacts). We derive such packings for  $n \leq 10$ , and provide a preliminary set of maximal contact packings for  $10 < n \leq 20$ . The resultant set of packings has some striking features, among them: (i) all minimally rigid packings for  $n \leq 9$  have  $3n - 6$  contacts, (ii) non-rigid packings satisfying minimal rigidity constraints arise for  $n \geq 9$ , (iii) the number of ground states (i.e. packings with the maximal number of contacts) oscillates with respect to  $n$ , (iv) for  $10 \leq n \leq 20$  there are only a small number of packings with the maximal number of contacts, and for  $10 \leq n < 13$  these are all commensurate with the HCP lattice. The general method presented here may have applications to other related problems in mathematics, such as the Erdos repeated distance problem and Euclidean distance matrix completion problems.

## 1. INTRODUCTION

We consider all configurations into which a set of  $n$  identical spheres in  $\mathbb{R}^3$  can pack by binding to each other. These sphere packings correspond to global and local maxima in the number of contacts – i.e. to structures in which either (i) no additional contacts between spheres can exist, or (ii) in order to form an additional contact, another contact must first be broken.

Our interest in answering this question arose through the desire to be able to direct the self-assembly of any given structure. This problem can be broken up into two parts: (i) the enumeration of all structures that can self-assemble for a given system, and (ii) directing the self-assembly of the system such that only the desired structure forms. Here we address (i), and (ii) is addressed in [5, 6].

As a model system, we chose to work with spherical colloidal particles because there are well known conditions under which small (nanometer to micron sized) spherical colloidal particles in solution will bind to one another, thereby causing them to self-assemble into structures [45, 35, 44, 10, 15, 21]. However, what all these structures are is unknown.

The attractive force that causes the binding between the particles, called a *depletion force*, is short-ranged, much smaller than the diameter of the particles themselves – small enough that the potential energy of a configuration of particles is linearly proportional to the number of contacts. The particles do not deform from their spherical shape, and can not overlap.

Mathematically, all possible structures into which such a system of  $n$  spherical colloidal particles can self-assemble correspond to all packings of  $n$  spheres in  $\mathbb{R}^3$  that can bind to one another. The enumeration of all possible self-assemblable structures for this system thus corresponds to the enumeration of all ‘sticky sphere packings’ – structures formed by spheres that pack via isotropic binding – here on in we will refer to these simply as sphere packings. We focus on enumerating only *minimally rigid* sphere packings; which we define as packings with  $\geq 3$  contacts per particle and  $\geq 3n - 6$  total contacts. Minimal rigidity is necessary, but not sufficient, for a structure to be rigid. We previously detailed the ground states of these packings, as well as reported some of

their interesting features in [7]. Here, we present the results and method more completely. The method we introduce combines graph theory and geometry to analytically derive all minimally rigid packings of  $n$  spheres. We perform this enumeration for  $n \leq 10$  spheres. Due to the large number of packings that must be evaluated, this analytical method is implemented computationally, and near  $n = 10$  we reach the method's computational limitations. Finding scalable methods for enumerating packings at higher  $n$  is a significant challenge for the future.

Already by  $n = 10$ , a number of interesting features set in. For  $n \leq 9$ , all minimally rigid packings have exactly  $3n - 6$  contacts. The first instance of a non-rigid sphere packing that satisfies minimal rigidity constraints occurs at  $n = 9$ , and more such non-rigid packings arise at  $n = 10$ . The first instance of packings with  $> 3n - 6$  contacts occurs at  $n = 10$ . We discuss the geometrical manner in which these maximal contact packings arise, and conjecture that all maximal contact packings for all  $n$  must contain octahedra. We provide preliminary evidence for this maximal contact conjecture for  $n \leq 20$ , and we show that the putative maximal contact packings of  $10 \leq n \leq 13$  are commensurate with the hexagonal close packing (HCP) lattice, but that maximal contact packings of  $14 \leq n \leq 20$  are not. Furthermore, we show that the number of packings containing the maximal number of contacts is oscillatory with  $n$ , and we discuss the origins of these oscillations.

The set of packings we enumerate include, as a subset, structures previously observed and described in the literature: for example, it includes all minimal-second-moment clusters reported by [43], and our construction provides a proof that these are the minimal-second-moment clusters<sup>1</sup> for  $n \leq 9$ . The set of packings we enumerate also includes those observed experimentally through capillary driven assembly of colloidal spheres [28, 35], as well as the Janus particle structures observed by Hong *et al.* [25].

This problem is also closely related to several unsolved problems in mathematics, such as the Erdos unit distance problem (a.k.a. the Erdos repeated distance problem), Euclidean distance matrix and positive semidefinite matrix completion problems, and 3 dimensional graph rigidity. Thus the method and results presented here may have direct bearing on these problems.

The organization of this paper is as follows: In the next section we outline our mathematical formulation of the problem and describe our methodology for finding all minimally rigid packings of a fixed  $n$ . We combine graph theoretic enumeration of adjacency matrices with solving for their corresponding distance matrices. The elements of these distance matrices correspond to the relative distances between spheres in 3 dimensional Euclidean space, and thus yield the packings that correspond to those adjacency matrices. Analytical methods for solving such adjacency matrices that scale efficiently with  $n$  do not exist. Sections 3 and 4 thus derive a method with improved scaling; which is divided into 2 parts, one of which scales efficiently for all  $n$ , and the other which requires new derivations at each  $n$ . Section 3 derives geometrical rules that map patterns in adjacency matrices either (i) to a configuration of spheres, in which case the adjacency matrix is solved for its corresponding distance matrix or matrices; or (ii) to an unrealizable configuration, in which case no real-valued embedding in 3 dimensional Euclidean space of that adjacency matrix exists in which spheres do not overlap. We show how these geometrical rules, combined with adjacency matrix enumeration, can lead to a provably complete set of minimally rigid packings. Each time a new pattern is encountered, a new geometrical rule must be derived; thus this part of the method requires new derivations at each  $n$ , and does not scale efficiently<sup>2</sup> with  $n$ . In section 4, we derive a single geometrical rule (the *triangular bipyramid rule*) that can

<sup>1</sup>[43] provided a proof for  $n \leq 4$ .

<sup>2</sup>Although this method does reach a higher  $n$  than is practical with current algebraic geometric methods.

solve all iterative adjacency matrices. An iterative adjacency matrix is an  $n \times n$  matrix in which all  $m < n$  subgraphs with  $\geq 3m - 6$  contacts also correspond to minimally rigid packings. This part of the method applies to any  $n$ , and thus scales efficiently for all  $n$ . Most adjacency matrices at small  $n$  are iterative; therefore, this greatly reduces the number of geometrical rules necessary to derive a complete set of packings. Section 5 describes the set of sphere packings we find from our study. We provide analytical formulas for packings up to  $n = 7$ , and the set of packings for  $n = 8, 9, 10$  are included in the supplementary information [8]. Section 6 summarizes notable properties of the packings, including how the number of contacts changes with  $n$ , the emergence of minimally rigid structures that are not rigid, and the emergence of maximal contact packings that are commensurate with lattice packings. Section 7 summarizes the main roadblocks towards obtaining results at higher  $n$  and contains several ideas and conjectures therein, and also discusses extensions to dimensions other than 3, as well as relevance to other problems of mathematical interest. Section 8 provides some concluding remarks.

## 2. MATHEMATICAL FORMULATION

We begin by presenting a two-step method for enumerating a complete set of sphere packings that satisfies minimal rigidity constraints. The set of all packings of  $n$  spheres is a subset of all possible configurations of  $n$  spheres. Thus, to enumerate a complete set of sphere packings we (i) use graph theory to enumerate all  $n$  sphere configurations, and (ii) determine which of those configurations correspond to sphere packings. The sphere packings we consider here correspond to maxima (local or global) in the number of contacts<sup>3</sup>. Provided step ii is exact, this method will produce a complete set of packings. However, current analytical methods do not scale efficiently with  $n$ , and are therefore ill-suited for step ii. Thus, in sections 3 and 4, we use basic geometry to derive an analytical method that can exactly determine which configurations correspond to sphere packings. Because the number of possible configurations grows exponentially with  $n$ , this analytical process must be implemented computationally. We focus our search to only those sphere packings satisfying minimal rigidity constraints ( $\geq 3$  contacts per sphere,  $\geq 3n - 6$  total contacts), because doing this guarantees that if a graph has an embedding in 3 dimensional euclidean space, it corresponds to a sphere packing; whereas graphs that are not minimally rigid can have 3 dimensional embeddings without corresponding to packings due to a continuous degree of freedom that allows for the formation of another contact.

We also note that spheres can be thought of as points (Fig. 1a,b), where points correspond to the centers of spheres, and we measure the distance between spheres as the distance between their centers. Throughout this paper we will use the words sphere, point, and particle interchangeably.

**2.1. Graph Theory Produces the Set of Possible Packings.** A configuration of  $n$  spheres can be described by an  $n \times n$  *adjacency matrix*,  $\mathcal{A}$ , detailing which spheres are in contact:  $\mathcal{A}_{ij} = 1$  if the  $i^{th}$  and  $j^{th}$  particles touch, and  $\mathcal{A}_{ij} = 0$  if they do not. A system of  $n$  spheres has  $n(n-1)/2$  interparticle distances; the 2 possibilities (touching or not touching) per distance thus leaves  $2^{n(n-1)/2}$  different ways of arranging contacts amongst the distances. There are thus  $2^{n(n-1)/2}$  possible adjacency matrices, each of which potentially corresponds to a packing.

Fig. 1 shows a packing of 6 particles, both as a sphere packing (Fig. 1a) and as points connected by line segments (Fig. 1b). The adjacency matrix corresponding to this packing is shown in Fig. 1c. The set of possible packings can be enumerated by considering *all adjacency matrices*.

---

<sup>3</sup>I.e. either the configuration of spheres can not form an extra contact (global maxima), or if an extra contact can be formed, it first requires the breaking of an existing contact (local maxima).

For  $n = 6$ , there are  $2^{15} = 32,768$  different adjacency matrices. Table 1 shows the number of adjacency matrices grows rapidly with  $n$ , reaching  $3.5184 \times 10^{13}$  by  $n = 10$ ; however, many of these correspond to the same structure due to particle labeling degeneracy. For example, switch labels 5 and 2 of Fig. 1; this yields another adjacency matrix corresponding to the same structure. Adjacency matrices corresponding to the same packing are *isomorphic* to one another – meaning there will exist a permutation of rows and columns that can translate one matrix into the other<sup>4</sup>.

To generate the complete set of possible packings, we need only enumerate *nonisomorphic*  $\mathcal{A}$ 's. Such algorithms exist; examples include *nauty* and the *SAGE* package called *nice* [36, 3]. The number of nonisomorphic matrices is much smaller but still grows exponentially with  $n$ . Table 1 shows this growth also; for example at  $n = 6$  the number of potential structures is 156, and at  $n = 10$  it is 12,005,168.

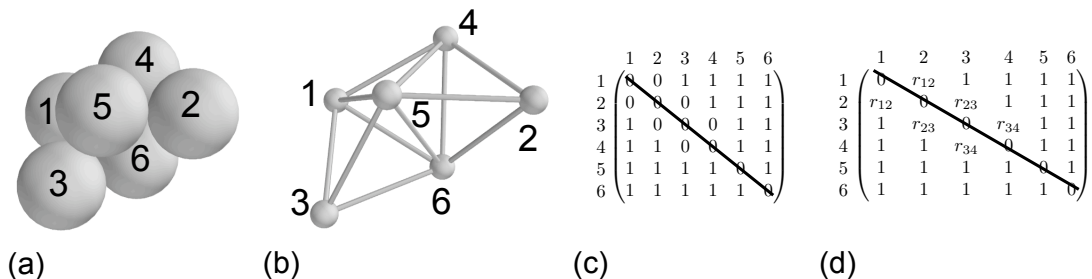


FIGURE 1. **Adjacency and Distance Matrix Representation of Packings.**

(a) 6 particle polytetrahedral sphere packing. (b) The same 6 particle packing shown in point/line representation. (c) Corresponding 6 particle adjacency matrix,  $\mathcal{A}$ . (d) Corresponding relative distance matrix,  $\mathcal{D}$ .

The set of  $\mathcal{A}$ 's (potential packings) can be greatly reduced by imposing rigidity constraints. Most structures with  $< 3n - 6$  total contacts or  $< 3$  contacts per particle will not correspond to a packing because there will exist a continuous degree of freedom through which the structure can form one or more bonds. Rigidity requires (i) there be at least 3 contacts per particle, and (ii) there be at least as many contacts as internal degrees of freedom – thus there must be at least  $3n - 6$  contacts<sup>5</sup>.

Table 1 shows how imposing minimal rigidity constraints restricts the number of adjacency matrices. For  $n \leq 5$  particles, this eliminates all but 1 adjacency matrix, thus identifying a unique packing for each of these  $n$ ; the doublet, triangle, tetrahedron, and triangular bipyramid, respectively. For  $n \leq 4$ , all relative distances within these packings are touching and are thus known. However, for  $n = 5$ , the packing contains one unknown relative distance, which must be solved. For  $n \geq 6$ , there exist  $> 1$  minimally rigid  $\mathcal{A}$ 's, and thus rigidity constraints alone are insufficient to identify the number of sphere packings (or to solve for them as  $> 1$  distance in each minimally rigid  $\mathcal{A}$  is unknown).

<sup>4</sup>See [23] for a nice example of such a permutation.

<sup>5</sup>Note that in restricting to structures with exactly  $3n - 6$  contacts, we will also find structures with  $\geq 3n - 6$  contacts. This is because when we actually solve for the packings as outlined below, the solutions can end up having more contacts than are assumed in the algebraic formulation.



**2.2. Solving Potential Packings: Algebraic Formulation.** To make further progress, we reformulate our problem algebraically. Each adjacency matrix element,  $\mathcal{A}_{ij}$ , is associated with an interparticle distance,

$$r_{ij} = \sqrt{(x_i - x_j)^2 + (y_i - y_j)^2 + (z_i - z_j)^2},$$

which is the distance between particles  $i$  and  $j$  whose centers are located at  $(x_i, y_i, z_i), (x_j, y_j, z_j)$ , respectively. The distances are constrained by the adjacency matrix as follows:

$$\begin{aligned} (1) \quad \mathcal{A}_{ij} &= 1 \implies r_{ij} = 2r \\ (2) \quad \mathcal{A}_{ij} &= 0 \implies r_{ij} \geq 2r \end{aligned}$$

where  $r$  is the sphere radius<sup>6</sup>.

For adjacency matrices with  $3n - 6$  contacts, this leads to precisely as many equations as unknowns<sup>7</sup>. The task is thus to solve for the  $r_{ij} \geq 2r$  given a particular set of  $r_{ij} = 2r$ . The particle configuration encoded by each  $\mathcal{A}$  is thus specified by a *distance matrix*,  $\mathcal{D}$ , whose elements  $\mathcal{D}_{ij} = r_{ij}$ .

The fundamental question is to find an efficient, exact method for mapping  $\mathcal{A} \rightarrow \mathcal{D}$ . If any  $\mathcal{D}_{ij} < 2r$ , this implies that particles  $i, j$  overlap; thus any  $\mathcal{D}$  with  $\mathcal{D}_{ij} < 2r$  is unphysical. Figure 1d shows the distance matrix corresponding to an  $n = 6$  packing. The interparticle distance between each of the particles that are touching is normalized to 1; for this packing, this leaves three distances to be solved;  $r_{12}, r_{23}$ , and  $r_{34}$ .

In solving  $\mathcal{A}$  for  $\mathcal{D}$ , the following scenarios are possible:

- (1) Continuous set(s) of real-valued  $\mathcal{D}$  correspond to a given  $\mathcal{A}$ , in which case the structure(s) are not rigid.
- (2) No real-valued  $\mathcal{D}$  exists that solves  $\mathcal{A}$ , in which case the structure is unphysical.
- (3) Finite, real-valued  $\mathcal{D}$  exist that solve  $\mathcal{A}$ . In this case, the structure(s) correspond to rigid sphere packing(s) provided that all  $\mathcal{D}_{ij} \geq 2r$ .

For every nonisomorphic adjacency matrix, whether there exists a corresponding packing requires solving for  $\mathcal{D}$  and asking whether the resulting  $r_{ij}$ 's satisfy these constraints.

**2.3. Limitations of Existing Solution Methods.** The issue now becomes one of solving a system of  $n(n-1)/2$  equations ( $3n-6$  equations and  $n(n-1)/2 - (3n-6)$  inequality constraints). Numerical approaches for solving these equations cannot be guaranteed to converge; for example, Newton's method requires an accurate initial guess for guaranteed convergence. When a solution does not converge, we do not know if it is because a solution does not exist, or because the initial guess is not sufficiently accurate. Algebraic geometric methods (e.g. Grobner bases) [11] are effective, but these algorithms do not scale efficiently with  $n$ . Our own implementation<sup>8</sup> of this method using the package *SINGULAR* [20] was only able to solve for structures up to  $n = 7$ .

In the following section, we use another approach and derive a different geometrical method to efficiently solve for all sphere packings given a set of nonisomorphic, minimally rigid  $\mathcal{A}$ 's. We

<sup>6</sup>Strictly speaking,  $A_{ij} = 0$  implies that particles are not touching, and thus that  $r_{ij} > 2r$ . However, it is convenient to consider all solutions of  $\mathcal{A}$ , which thus include the possibility  $r_{ij} = 2r$  for  $\mathcal{A}_{ij} = 0$ ; in other words, a packing can be represented by multiple  $\mathcal{A}$ 's with different numbers of 1's if the solution to  $A_{ij} = 0$  forces it to a 1.

<sup>7</sup>Without loss of generality, we can set one particle to reside at the origin, another to reside along a single axis (for example the  $y$ -axis), and a third to reside in one plane (such as the  $xy$ -plane) – 6 coordinates are then fixed, leaving  $3n - 6$  instead of  $3n$  coordinates.

<sup>8</sup>At  $n = 8$ , using the software package *SINGULAR* [20], one matrix takes several hours to solve, and there are a total of 438 minimally rigid non-isomorphic  $\mathcal{A}$ 's.

$n$	$\mathcal{A}$ 's	Non-Isomorphic $\mathcal{A}$ 's	Minimally rigid $\mathcal{A}$ 's	Iterative $\mathcal{A}$ 's	Non-Iterative $\mathcal{A}$ 's
1	1	1	1	1	0
2	2	2	1	1	0
3	8	4	1	1	0
4	64	11	1	1	0
5	1,024	34	1	1	0
6	32,768	156	4	3	1
7	2,097,152	1,044	29	26	3
8	268,435,456	12,346	438	437	1
9	$6.8719 \cdot 10^{10}$	274,668	13,828	13,823	5
10	$3.5184 \cdot 10^{13}$	12,005,168	750,352	750,226	126

TABLE 1. **The Growth of Adjacency Matrices with  $n$ .**

The number of adjacency matrices (constructed by [36]) decreases rapidly as isomorphism and rigidity constraints are imposed. Iterative and non-iterative are defined in the text. The classification of whether an  $\mathcal{A}$  is iterative or not is here shown after all rules for  $n - 1$  particles are applied; thus the non-iterative column shows  $n$  particle non-iterative structures only, and does not include  $< n$  particle non-iterative structures.

implement this method up to  $n = 10$ , at which point we begin to hit some roadblocks; these are discussed at the end of the paper, where we outline potential ways to overcome them.

**2.3.1. Chiral Structures and Enantiomers.** Before proceeding further, it is worth remarking that structures with different handedness will correspond to the same distance matrix. We can analyze each  $\mathcal{D}$ , and determine whether it corresponds to a structure that has a chiral counterpart or an enantiomer (see section 3.4). We refer to chiral structures as the same packing but different states – thus, a distance matrix having a left- and right-handed counterpart corresponds to 1 packing with 2 different states. Note that according to our definition, a different packing necessarily corresponds to a different state. Thus, the total number of states is equal to the total number of packings plus the total number of chiral counterparts.

### 3. GEOMETRICAL RULES SOLVE FOR SPHERE PACKINGS

We now show how geometrical rules can be used to effectively and analytically solve the class of polynomial equations that are generated by adjacency matrices. We use basic geometry to construct rules associating patterns of 1's and 0's in  $\mathcal{A}$ 's with either a given relative distance,  $\mathcal{D}_{ij}$ , or an unphysical conformation (in which case no  $\mathcal{D} \geq 2r$  exists). There thus exist two types of rules: *Elimination rules* eliminate an  $\mathcal{A}$  as unphysical, and *distance rules* solve an  $\mathcal{A}_{ij}$  for its corresponding  $\mathcal{D}_{ij}$ .

**3.1. Neighbor Spheres and Intersection Circles.** With each sphere of radius  $r$ , we can associate a *neighbor sphere* of radius  $R = 2r$ , whose surface defines where another sphere must lie if it is to touch the original sphere in question (Fig. 2a). When 2 spheres touch, their neighbor spheres intersect in an *intersection circle* (Fig. 2b). The radius of the intersection circle follows from straightforward geometry, and is  $\frac{\sqrt{3}}{2}R$  (see supplemental information for derivation [8]).

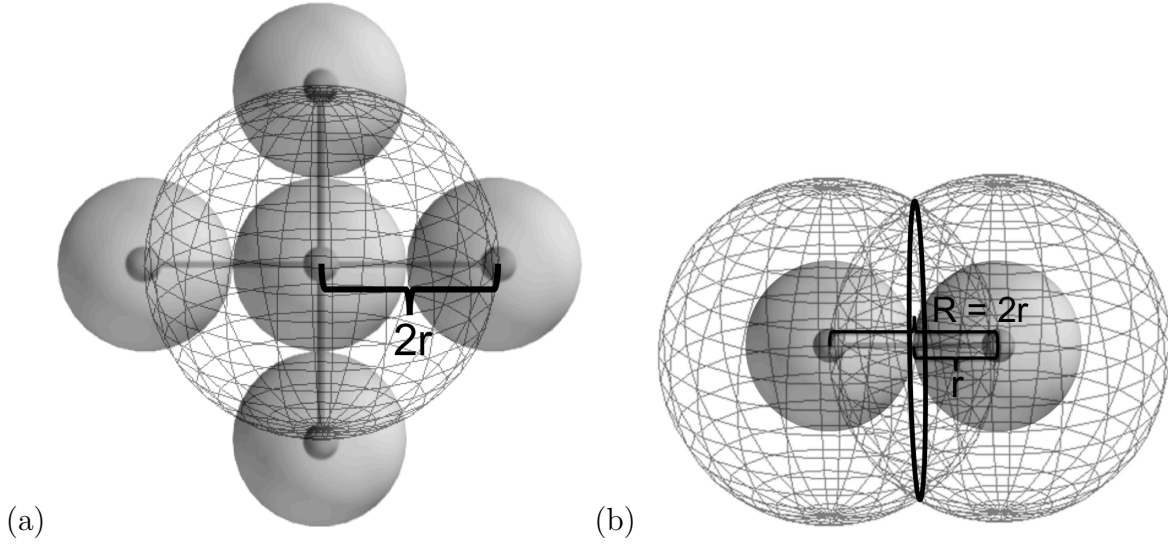


FIGURE 2. **The Neighbor Sphere.**

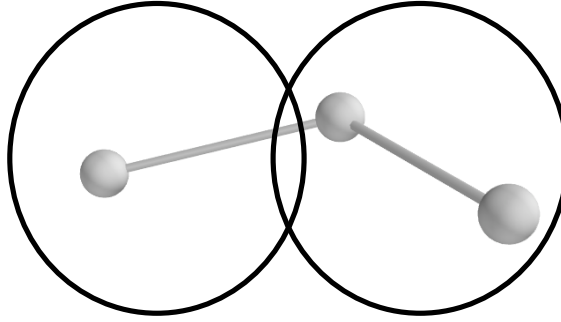
(a) A particle and its neighbor sphere. 4 particles are shown touching the center particle, and it is seen that their centers lie on the surface of the particle's neighbor sphere. (b) 2 touching particles. The associated neighbor spheres of the particles intersect in an *intersection circle* of radius  $(\sqrt{3}/2)R$ .

Now we can interpret each  $\mathcal{A}_{ij} = 1$ , in geometrical terms, as an intersection circle between spheres  $i$  and  $j$ . Minimal rigidity constraints imply that each particle is associated with at least 3 intersection circles. Intersection circles can be used to derive geometrical rules because, in general, a packing of  $n$  particles involves intersections of intersection circles, and intersections of intersection circles define points in space. A particle touching  $m$  other particles will lie at the intersection of those  $m$  neighbor spheres. For example, a particle touching the dimer depicted in figure 2b will lie on the circumference of the associated intersection circle. The intersection of  $m \geq 3$  neighbor spheres are points – and by defining points in space, basic trigonometry can be used to calculate the distances between those points, thus solving  $\mathcal{A}$ 's for  $\mathcal{D}$ 's.

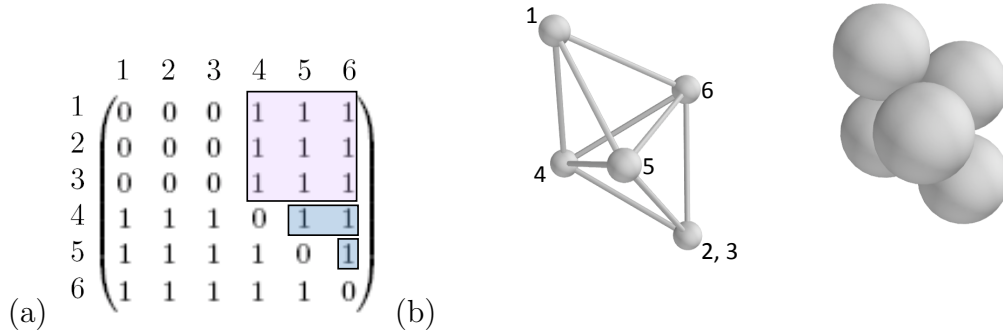
**3.2. Individual Geometrical Rules.** Using intersection circles, we now derive several representative geometrical rules for eliminating and solving adjacency matrices. The supplementary information [8] contains the complete set of rules used to derive the results of this paper.

**3.2.1. Rule 1.** The simplest rule arises from the fact that intersection circles can intersect in either 2, 1 or 0 points, but never more than 2 points. This geometrical fact implies that any  $\mathcal{A}$  with the following property is unphysical: any 2 of the set  $\{\mathcal{A}_{jk}, \mathcal{A}_{jp}, \mathcal{A}_{kp}\}$  equal 1, and  $\exists > 2$   $i$ 's for which  $\mathcal{A}_{ij} = \mathcal{A}_{ik} = \mathcal{A}_{ip} = 1$ .

Physically, this implies that no more than 2 spheres can touch 3 linearly connected spheres (Fig. 3); which in turn tells us how many identical spheres can mutually touch a trimer: 2. Figure 4 shows an example of an adjacency matrix that is unphysical for this reason: the blue highlighted section shows that spheres 4,5,6 make up a trimer; but the purple highlighted section shows that spheres 1,2,3 all touch the same trimer. This is impossible given the argument outlined above and hence this adjacency matrix does not correspond to a packing.



**FIGURE 3. No More than 2 Particles can Touch 3 Connected Particles.** Schematic of 3 linearly connected particles and their associated intersection circles. The center of each intersection circle lies at the midpoint of the line segment connecting the associated points. There can never be  $> 2$  intersection points of these intersection circles, indicating that no more than 2 particles can touch the same 3 linearly connected particles.



**FIGURE 4. Example of an Unphysical Adjacency Matrix.** (a) An adjacency matrix that is unphysical because it implies  $> 2$  intersections of intersection circles. The blue highlights show that particles 4,5,6 make up a trimer. The purple highlighted part shows that particles 1, 2, and 3 all touch the same trimer, 4,5,6. (b) A sphere packing to which this unphysical adjacency matrix corresponds (shown in both sphere and point/line representations). For it to be realized, it implies that 2 particles must occupy the same point in space.

**3.2.2. Rule 2.** A trimer is associated with 3 mutually intersecting intersection circles (Fig. 5a). These 3 intersection circles intersect at 2 points (shown in red). Here we calculate the distance between these 2 intersection points.

Note that a particle lying at one of the intersection points forms the 4 particle packing (the tetrahedron). And that 2 particles, lying at each intersection point, form the 5 particle packing (the 5 point polytetrahedron). The distance between these 2 intersection points,  $h$ , is the only distance  $> R$  in the 5 particle packing (Fig. 6).

To calculate this distance, we note that the trimer and its associated intersection circles form the set of triangles shown in Fig. 5b (where the dashed line indicates an out-of-plane triangle). We calculate  $a$  by considering the right triangle with sides  $\sqrt{3}/2 R - a, a, 1/2 R$ . Trigonometry then implies that  $a = R/(2\sqrt{3})$ , and  $h = 2\sqrt{2/3}R$ .

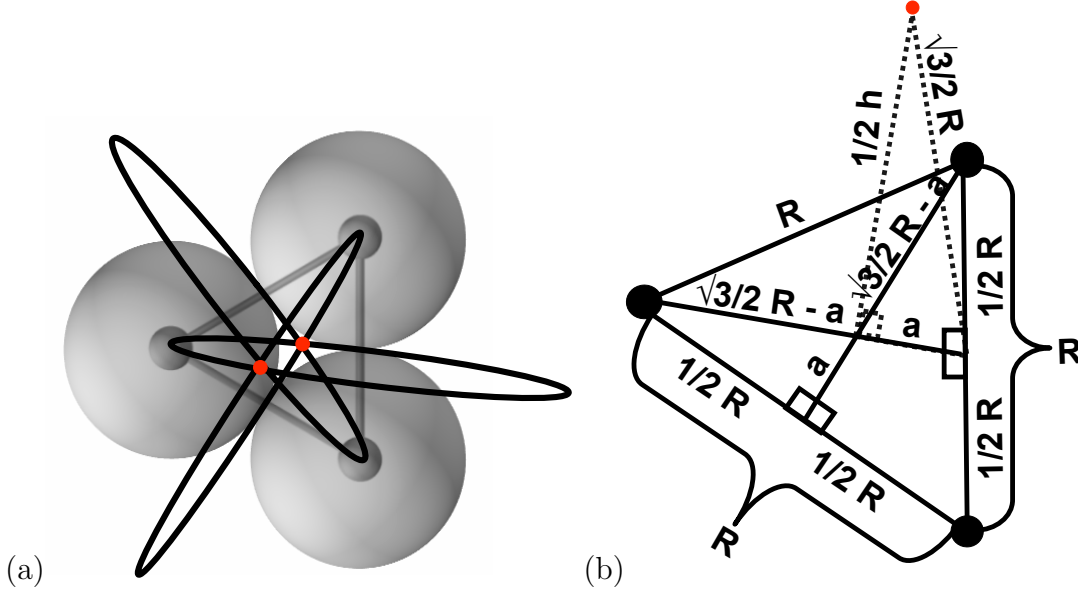


FIGURE 5. **The Intersections of 3 Intersection Circles.**

(a) A trimer and its corresponding intersection circles. The 3 intersection circles mutually intersect at 2 points, shown in red. (b) The triangles that relate the trimer to one of the points of intersection (red dot). The distance between this point and the center of the triangle is equivalent to half the distance between the 2 points of intersection.

This implies that the solution to an adjacency matrix corresponding to the 5 particle packing is

$$\begin{pmatrix} 0 & 1 & 1 & 1 & 1 \\ 1 & 0 & 1 & 1 & 1 \\ 1 & 1 & 0 & 1 & 1 \\ 1 & 1 & 1 & 0 & 0 \\ 1 & 1 & 1 & 0 & 0 \end{pmatrix} \rightarrow \begin{pmatrix} 0 & 1 & 1 & 1 & 1 \\ 1 & 0 & 1 & 1 & 1 \\ 1 & 1 & 0 & 1 & 1 \\ 1 & 1 & 1 & 0 & 2\sqrt{\frac{2}{3}} \\ 1 & 1 & 1 & 2\sqrt{\frac{2}{3}} & 0 \end{pmatrix}$$

where the right matrix is the corresponding distance matrix,  $\mathcal{D}$ . For  $n = 5$ , there is only 1 non-isomorphic minimally rigid  $\mathcal{A}$ .

We can formalize this construction as a distance rule, which can be used whenever a submatrix of some  $\mathcal{A}$  has the same structure as the 5 particle packing. Such submatrices can be identified with

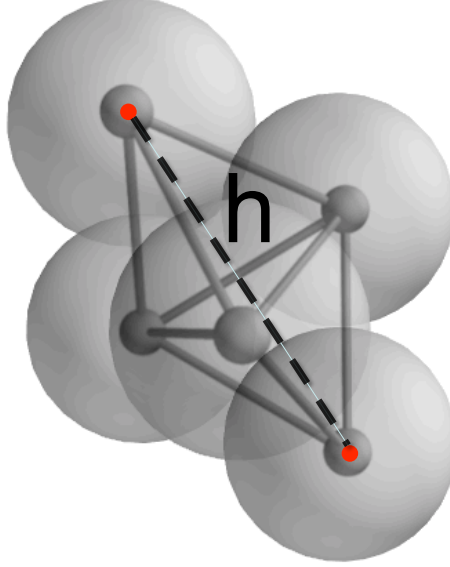


FIGURE 6. **The 2 Intersection Points of a Trimer Correspond to the 5 Particle Packing.** A 5 particle packing is shown with its point representation overlain. The center triangle of the point representation corresponds to a trimer, and the 2 points that contact the trimer correspond to the 2 intersection points of the trimer's 3 intersection circles. The 2 intersection points are shown in red, and  $h$  corresponds to the distance between them.

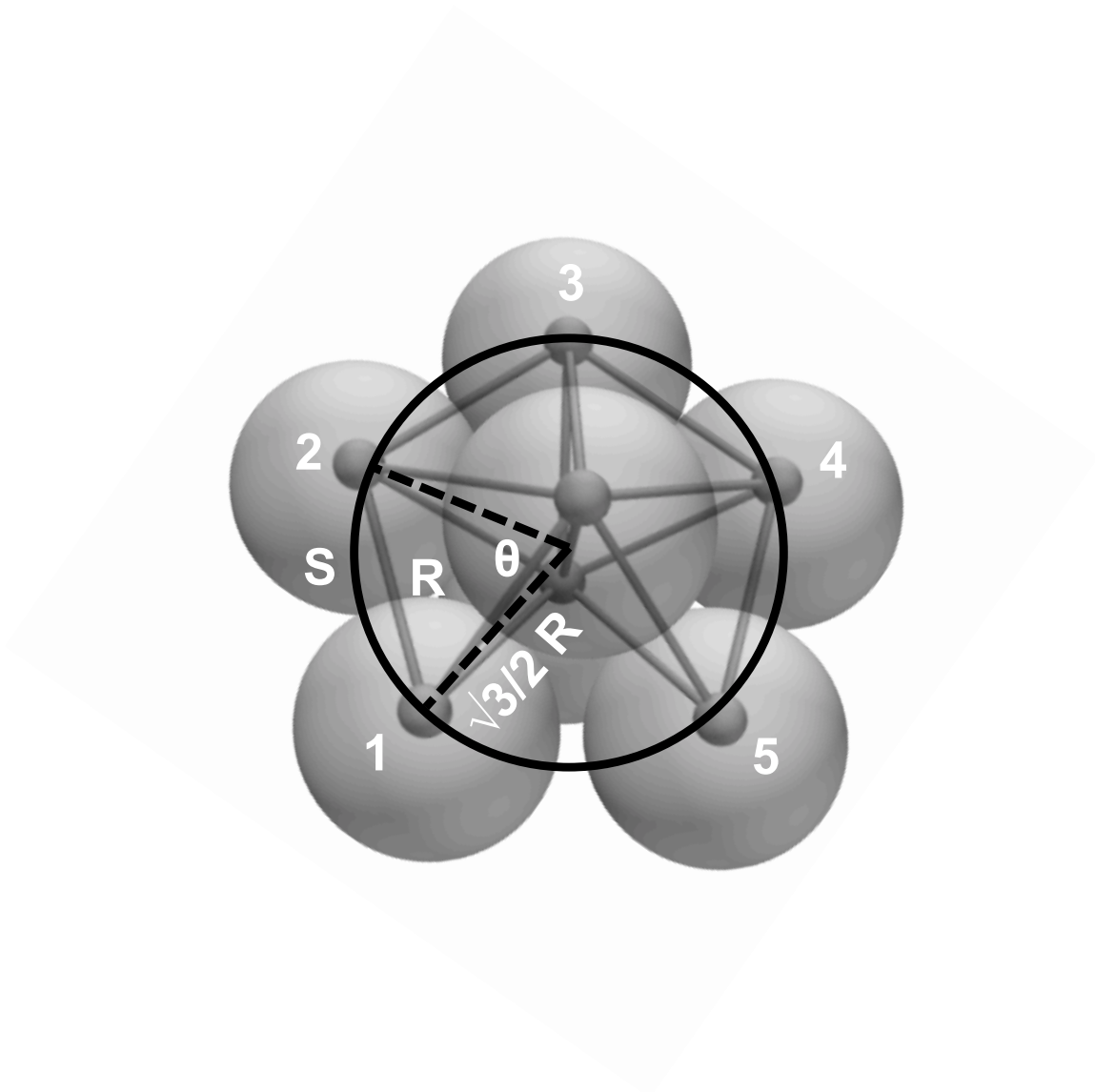
the following pattern:  $\mathcal{A}_{ij} = \mathcal{A}_{ik} = \mathcal{A}_{kj} = 1$ , and  $\exists 2 p$  for which  $\mathcal{A}_{pi} = \mathcal{A}_{pj} = \mathcal{A}_{pk} = 1$ . Whenever this pattern exists, the distance sub-matrix between the corresponding points corresponds to  $\mathcal{D}$  for the 5 particle packing. In particular, this rule solves for the distance between the 2  $p$ , for example if  $p = l, m$ , then  $\mathcal{D}_{lm} = 2\sqrt{\frac{2}{3}}R$ .

**3.2.3. Rule 3.** Another elimination rule follows directly from any distance rule, including Rule 2 derived above. Suppose we determine that for a given pattern of  $\mathcal{A}_{ij}$ , the contact distribution implies that  $\mathcal{D}_{kp} > R$ . If it then happens that  $\mathcal{A}_{kp} = 1$ , then this implies that all of the geometrical constraints cannot be satisfied simultaneously, so that  $\mathcal{A}$  is unphysical.

For example, if an  $\mathcal{A}$  contained the intersection circle construction discussed in the previous section, that would imply that  $\mathcal{D}_{lm} = 2\sqrt{2/3}R$ , but if the adjacency matrix also stated that  $\mathcal{A}_{lm} = 1$ , then that  $\mathcal{A}$  would be unphysical.

**3.2.4. Rule 4.** We can derive another set of geometrical rules by finding the maximum number of points that can lie on an intersection circle – this corresponds to the maximum number of spheres

that can touch a dimer. Fig. 7 shows the dimer (top and bottom black spheres), as well as points lying on their intersection circle.



**FIGURE 7. 5 Points on an Intersection Circle.**

The intersection circle shown in black corresponds to the dimer in the center. 5 points are shown lying on the intersection circle; this corresponds to 5 particles touching the center dimer. The radius of the intersection circle is  $(\sqrt{3}/2)R$  (shown as dashed black lines), and connects the center of the dimer (which is the origin of the intersection circle) to points 1-5 on the intersection circle.  $S$  is the arc length swept out by one pair of particles on the intersection circle. It can be seen that the 1st and 5th particles nearly touch. The space between them is not big enough to fit another particle, and thus it can be seen that no more than 5 particles can touch a dimer.

The maximum number of spheres that can lie on an intersection circle is 5, and this can be calculated as follows: we divide the circumference of the entire intersection circle by the arc length swept out by 2 spheres lying a unit distance apart<sup>9</sup> (see figure 7). This arc length is given by  $S = r\theta$ , where  $r$  is the radius of the intersection circle, and  $\theta$  is the angle between 2 radial line segments. The law of cosines then implies that

$$(3) \quad \theta = \cos^{-1} \left( \frac{1}{3} \right),$$

so that the number of points a distance  $R$  apart that can fit on an intersection circle is given by

$$(4) \quad \frac{2\pi \frac{\sqrt{3}}{2} R}{\frac{\sqrt{3}}{2} R \cos^{-1} \left( \frac{1}{3} \right)} \approx 5.1043.$$

This indicates that (i) any  $\mathcal{A}$  implying  $> 5$  points lie on an intersection circle, and (ii) any  $\mathcal{A}$  implying a unit distance between all  $m \leq 5$  points lying on an intersection circle is unphysical. We can identify 5 points lying on an intersection circle by the following adjacency matrix pattern:  $\mathcal{A}_{ij} = 1$ , such that there are  $> 5$   $k$  for which  $\mathcal{A}_{ik} = \mathcal{A}_{jk} = 1$ .

To solve for the structure of  $m \leq 5$  points lying on an intersection circle, we must compute the distances between the non-touching particles on the intersection circle (Fig. 7). Of these distances, we have already calculated that between points 1 and 3 and shown that it is  $= 2\sqrt{2/3}R$  (section 3.2.2). All of these distances can be obtained by the isosceles triangle with equivalent lengths  $\sqrt{3}/2R$  (corresponding to the dashed black lines in Fig. 7 – note that only 2 such lines are shown, but that they exist between the midpoint of the dimer and every point along the intersection circle). The unique length of the isosceles triangle will be the unknown distance,  $r_{ij}$ , and the angle between the two  $\sqrt{3}/2R$  sides connecting particles  $i$  and  $j$  will be called  $\phi_{ij}$ . Thus, the unknown distances will all be given by

$$(5) \quad \sin \left( \frac{1}{2} \phi_{ij} \right) = \frac{\frac{1}{2} r_{ij}}{\frac{\sqrt{3}}{2} R}$$

where

$$\begin{aligned} \phi_{13} &= 2\theta \\ \phi_{14} &= 2\pi - 3\theta \\ \phi_{15} &= 2\pi - 4\theta \end{aligned}$$

where  $\theta$  is given by eqn 3, thus yielding

$$(6) \quad r_{13} = 2\sqrt{\frac{2}{3}}R$$

$$(7) \quad r_{14} = \frac{5}{3}R$$

$$(8) \quad r_{15} = \frac{4\sqrt{6}}{9}R$$

These calculations apply to any adjacency matrix with the following structure: If  $\mathcal{A}_{ij} = 1$ , and  $\exists n$   $k$  for which  $\mathcal{A}_{ik} = \mathcal{A}_{jk} = 1$ , and  $n - 1$   $\mathcal{A}_{pq} = 1$  amongst the  $n$   $k$ , where  $n = 3, 4, 5$  for  $r_{13}, r_{14}, r_{15}$ , respectively. Then the distance between the two endpoints of the  $n$  particles is given

---

<sup>9</sup>Without loss of generality, we refer to the distance between two touching spheres,  $R$ , as the unit distance.



by  $\mathcal{D}_{pk} = r_{13}, r_{14}, r_{15}$ , respectively.

I.e. for

$n = 2$ : if  $k = p, q, l$ , then  $\mathcal{A}_{pq} = \mathcal{A}_{ql} = 1$ , and the distance  $\mathcal{D}_{pl} = 2\sqrt{\frac{2}{3}}R$ .

$n = 3$ : if  $k = p, q, l, m$ , then  $\mathcal{A}_{pq} = \mathcal{A}_{ql} = \mathcal{A}_{lm} = 1$ , and the distance  $\mathcal{D}_{pm} = \frac{5}{3}R$ .

$n = 4$ : if  $k = p, q, l, m, z$ , then  $\mathcal{A}_{pq} = \mathcal{A}_{ql} = \mathcal{A}_{lm} = \mathcal{A}_{mz} = 1$ , and  $\mathcal{D}_{pz} = \frac{4\sqrt{6}}{9}R$ .

Note for  $n = 3$ , we have already identified this  $\mathcal{A}$  pattern in section 3.2.2, whereas the  $n = 2, 4$  structures are new. Also note that, by symmetry,  $r_{13} = r_{24} = r_{35}$ , and  $r_{14} = r_{25}$ , and that these equivalences are identified by the above patterns in  $\mathcal{A}$ .

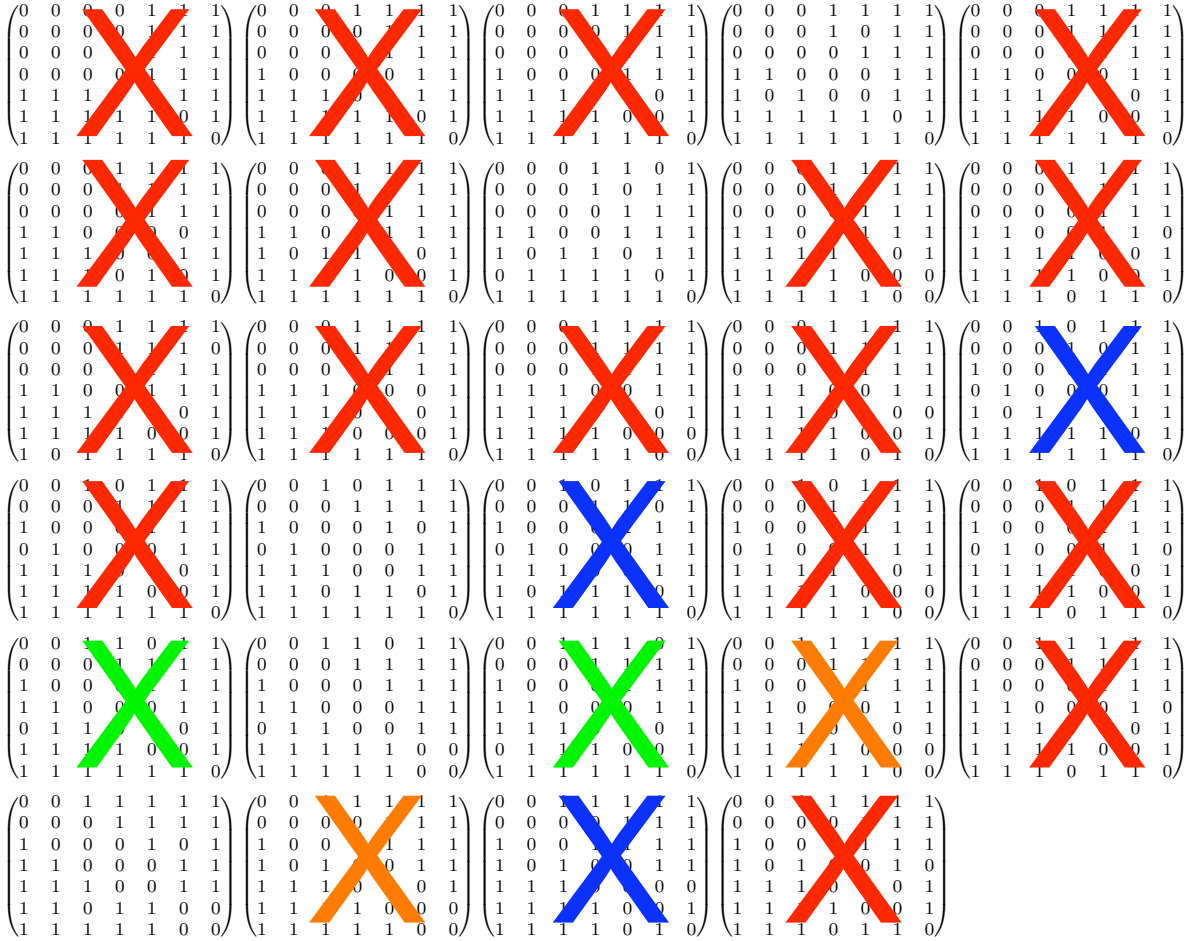


FIGURE 8. **Eliminating Adjacency Matrices.** There are 29 non-isomorphic adjacency matrices satisfying minimal rigidity constraints for 7 particles. 24 out of the 29  $\mathcal{A}$ 's are eliminated by geometrical rules, which are shown here as color-coded **X**'s – see table 2 and appendix A for the corresponding rules. See Fig. 9 for solutions to the 5 physically realizable  $\mathcal{A}$ 's.

**3.3. Using Geometrical Rules to Derive a Complete Set of Sphere Packings.** The aforementioned geometrical rules can be used, along with the set of nonisomorphic adjacency matrices

for a given  $n$ , to derive a complete set of packings. To explain more clearly how this is done, we show as an example the complete derivation for  $n = 7$  particle packings. For this  $n$ , there exist 29 minimally rigid potential packings, derived by asking how many nonisomorphic  $n = 7$  adjacency matrices have  $3n - 6 = 15$  contacts and 3 contacts per particle.

To these matrices, we apply the elimination rules just outlined, as well as those that appear in the supplementary information [8]. This immediately eliminates 24/29  $\mathcal{A}$ 's as unphysical. Figure 8 shows which of the matrices are eliminated. Table 2 shows which rules are used to eliminate the  $\mathcal{A}$ 's. 17/24 of the matrices are eliminated because they imply  $> 2$  intersections of intersection circles. Three of the matrices are eliminated because of the relative distance rule for three points on an intersection circle. Two matrices each are eliminated by rules acting on 5 rings and 4 rings, respectively. For the remaining five adjacency matrices, we apply distance rules to the  $\mathcal{A}$ 's to solve for the corresponding  $\mathcal{D}$ 's. Table 3 details which distance rules are used to solve each  $\mathcal{A}$ . The analytical solutions for the distance matrices as well as the associated packings are shown in Fig. 9; to each  $\mathcal{A}$  (numbered by the order in which it appears in Fig. 8, in ascending order from left to right, and top to bottom, respectively), we apply the rules outlined in Table 3 to analytically solve for the packing.

**TABLE 2. Elimination Rules Used for 7 Particle Packings.**

Each rule appears in its own section either in the text or in appendix A, where the complete set of rules is included. The rule column thus lists in what section(s) the relevant rules can be found.

Color:	Unphysical Because:	Rule:
<b>X</b>	2 or more intersection circles intersect at $> 2$ points	A.1 section 3.2.1
<b>X</b>	All relative distances between 3 points lying on an intersection circle $= R$	A.3 sections 3.2.2, 3.2.3 and 3.2.4
<b>X</b>	A closed 5 ring surrounds a circle of intersection	A.14
<b>X</b>	2 points on opposite sides of a closed 4 ring touch	A.15

**TABLE 3. Rules Needed to Solve 7 Particle Packings.**

The rules listed here correspond to distance rules. Rule 'A.#' corresponds to rule # in appendix A, otherwise the relevant equation and section numbers are listed for rules found within the paper. (Note that rule 4, found in section 3.2.4 (eqn 6), is the same as rules 2 (section 3.2.2) and A.1, rule 4 (eqn 7) is the same as rule A.2, and rule 4 (eqn 8) is the same as rule A.4). Graphs are numbered in ascending order from left to right and top to bottom as they appear in Fig. 8. These graphs correspond to the ones without **X**'s.

Graph Number:	Rules Used:
4	section 3.2.4 eqns 6, 7, and 8
8	section 3.2.4 eqns 6 and 7
17	section 3.2.4 eqns 6, 7; and A.11
22	A.7 and A.6
26	A.3 and A.9

This is the provably complete set of 7 particle sphere packings. Note that the packing corresponding to graph 17 (row 4 from the top) is the only one where distinct left and right handed structures are possible; thus it corresponds to 2 distinct states.

**3.4. Enantiomers and Chirality.** Once all packings have been derived by solving all  $\mathcal{A}$ 's for their corresponding  $\mathcal{D}$ 's, we must determine how many states each packing has. If a packing is chiral, it will have more than one state. This will show up by a packing having different 'handedness;' for example, a packing with a mirror image that is non-superimposable will have distinct left and right-handed structures, and thus have 2 distinct states. We will proceed with the following definitions: an enantiomer corresponds to a structure that has a non-superimposable mirror image (i.e. a non-superimposable reflection across the  $x, y$ , or  $z$  plane); a chiral structure corresponds to a structure that has a non-superimposable image across any plane of symmetry. Thus, defined in this manner, enantiomers are a subset of chiral structures, and we will therefore proceed by referring to structures as chiral alone.

One can calculate whether a packing is chiral as follows: The automorphism group of a packing,  $\{\alpha\}$ , gives the set of self-isomorphisms – i.e. all possible permutations of the structure into itself. Each element of the automorphism group will thus correspond either to a rotation or to a reflection. Rotations are transformations with determinant = 1, and reflections are transformations with determinant = -1. Thus, one can construct the set of all isomorphic graphs,  $\{\mathcal{D}\}$ , and construct the automorphism group for any one  $\mathcal{D}_i$  within the isomorphic set. If  $\exists$  any matrix  $\mathcal{D}_j \in \{\mathcal{D}\}$  that is isomorphic to  $\mathcal{D}_i$  *only* through reflections and not through rotations – i.e. if the isomorphism group of  $\mathcal{D}_j$  to  $\mathcal{D}_i$  corresponds to transformations that all have determinant -1, then the packing  $\mathcal{D}$  is chiral.

A property related to chirality is the symmetry number,  $\sigma$ . This corresponds to the number of ways that a structure can be rotated into itself. The symmetry is necessary for calculating the equilibrium probability distribution of packings [5, 37]. The symmetry number of a packing,  $\mathcal{D}$ , will be equal to the number of transformations within the automorphism group of  $\mathcal{D}$  that have determinant 1. Thus, if a packing has no reflections, then the symmetry number will simply equal the size of the automorphism group. If a packing has reflections, then the symmetry number will equal the size of the automorphism group divided by 2 (dividing by 2 will remove all automorphism mappings corresponding to reflections, and not rotations).

Related to both symmetry numbers and chirality are point groups. A point group is a group of symmetry operations which all leave at least one point unmoved. Point groups have been calculated for many structures – and there exist programs that allow one to enter in a set of coordinates and retrieve the point group corresponding to those coordinates [41]. Symmetry numbers and chirality can alternatively be calculated directly from the point group of a structure. For example, compounds in the  $C_m$  point group, where  $C_m$  is the cyclic group consisting of rotations by  $360^\circ/m$  and all integer multiples (where  $m$  is an integer), are always chiral [22].

Point groups, symmetry numbers, and chirality of packings are included in the lists of packings appearing in section 5 and in the supplementary information [8]. The growth of chiral structures with  $n$  is interesting – surprisingly, over half of all 9 particle packings are chiral – see table 4.

#### 4. ONE GEOMETRICAL RULE THAT SOLVES FOR ALL ITERATIVE PACKINGS: THE TRIANGULAR BIPYRAMID RULE

In principle, these types of geometrical rules can be used to derive a complete set of sphere packings for any number of particles,  $n$ . However, in practice, the number of rules used here grows too quickly with  $n$  for this to be a practical method: at  $n = 5$  spheres, only 1 rule is

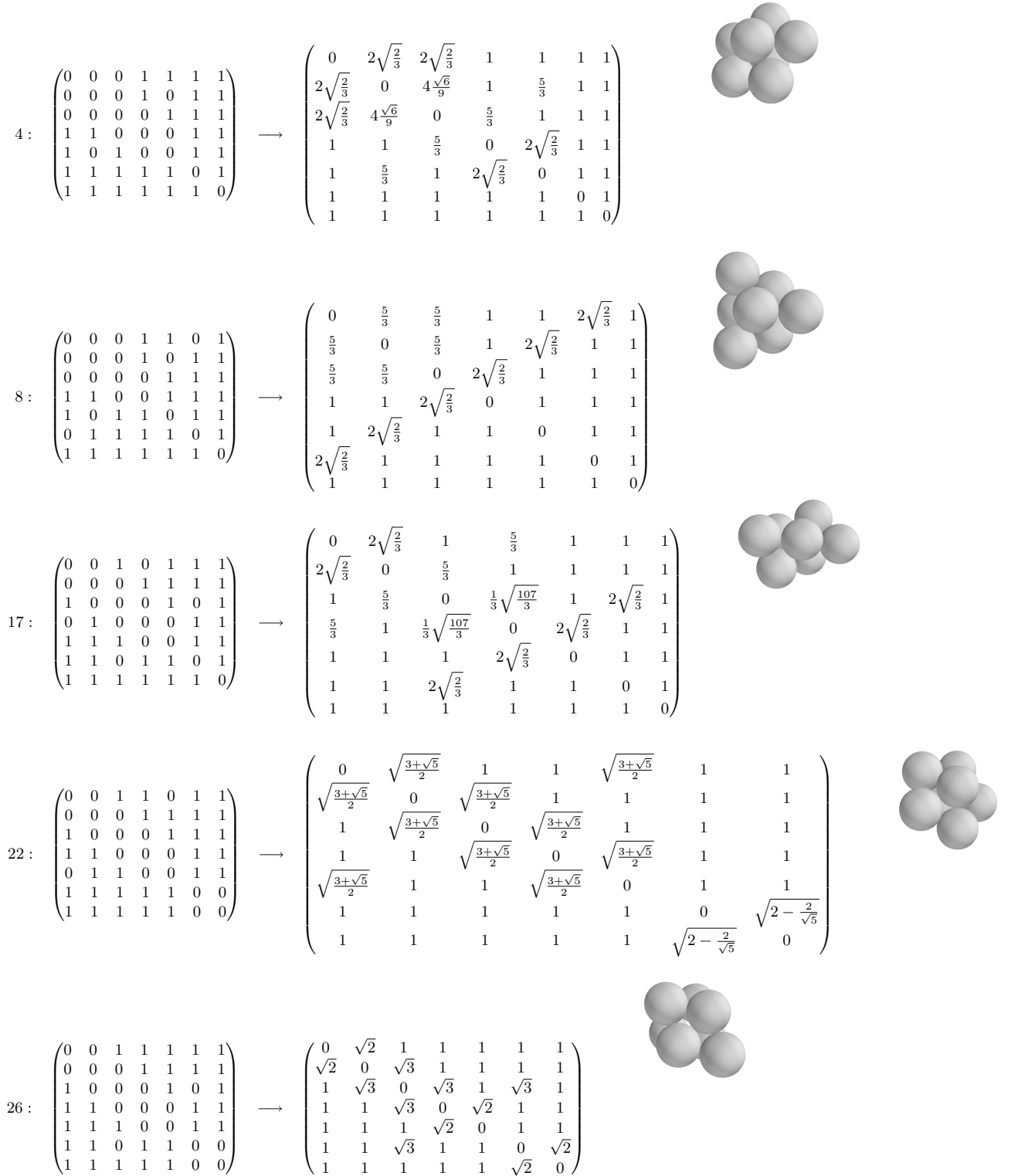


FIGURE 9. 7 Particle Packings.

These are the 5 possible packings of 7 particles. Graph numbers appear to the left – corresponding to a sequential numbering of the graphs appearing in Fig. 8 from left to right and top to bottom, respectively. Following the graph numbers are  $\mathcal{A}$ ,  $\mathcal{D}$ , and a picture of the corresponding packing, respectively. Note that graph 17 is chiral – it has both a left-handed and a right-handed form (this can be seen by moving the top particle to the other side).

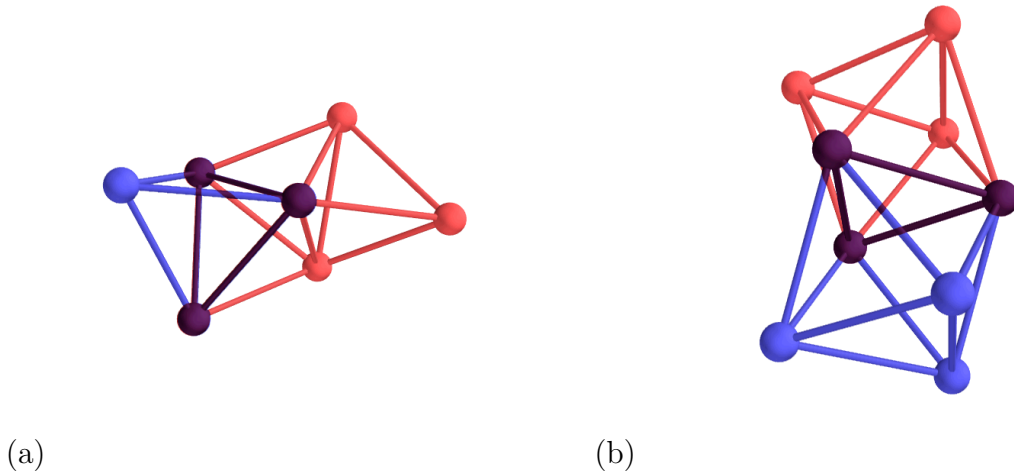


FIGURE 10. **Iterative Packings.** Two examples of iterative packings. (a) A 6 particle polytetrahedron (red) with one particle added to it (blue). This decomposes into a tetrahedron (blue) plus a 6 particle polytetrahedron (red), with a shared triangular base (purple). (b) 2 joined octahedra (one red and one blue, with a shared purple triangular base) forming a 9 particle packing.

required, 3 rules are needed at  $n = 6$ , 12 rules at  $n = 7$ , and at  $n = 8$ , 14 rules solve 435/438 minimally rigid non-isomorphic  $\mathcal{A}$ 's. This leaves 3 unsolved  $\mathcal{A}$ 's for which more geometrical rules must be derived; looking ahead at the 13,828 and 750,352  $\mathcal{A}$ 's that must be solved at  $n = 9, 10$ , respectively, it becomes clear that deriving a rule or set of rules that does not grow significantly with  $n$  is a necessary step. Here, we derive one geometrical rule that can solve one class of packings for any  $n$ , thereby greatly reducing the number of rules needed to derive a complete set of  $n$  sphere packings. In section 7.2, we discuss how one geometrical rule can also be used to solve the other class of packings for all  $n$ .

Packings can be broken up into two types or classes: *iterative* and non-iterative, or *new seeds*. Iterative packings are  $n$  particle packings that are solely combinations of  $< n$  particle packings (see Fig. 10). New seeds, are  $n$  particle packings that can not be constructed solely out of  $< n$  particle packings – i.e. they contain within them (in part or in whole) an inherently new structure (Fig. 11). Put another way, iterative packings correspond to  $\mathcal{A}$ 's for which all minimally rigid  $m$  x  $m$  subgraphs,  $m < n$ , correspond to packings that have been identified at lower  $n$ .

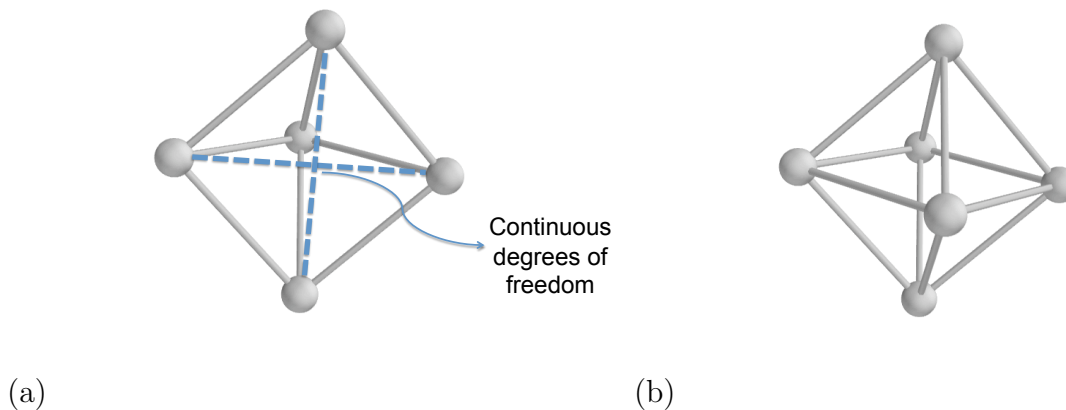


FIGURE 11. **New Seeds.** The octahedron is an example of a new seed. (a) The ‘base’ of an octahedron – it has a continuous degree of freedom through which a 5 particle polytetrahedron can form, and thus is not a packing. The continuous degrees of freedom are shown as dashed lines; bringing either of the pairs of particles connected by these dashed lines into contact forms the 5 particle polytetrahedron. (Note that the 5 particle structure shown in (a) is not minimally rigid as it has  $< 3n - 6 = 12$  contacts.) (b) Once a 6th particle is added, the octahedral structure can be stabilized, thereby forming a *new seed*. This ‘new seed’ is an inherently new structure.

**4.1. Solving iterative structures.** An iterative packing is a polyhedron comprised *solely* of  $< n$  particle packings<sup>10</sup>. Thus any iterative packing can be decomposed into 2 joined polyhedra (see fig 10 – the red and blue packings are the joined polyhedra). The 2 polyhedra are joined via a common base of particles (shown in purple)<sup>11</sup>. Because the joined polyhedra are  $< n$  particle packings, all of their *intrapolyhedral* distances are known from lower order packings.

Thus, deriving one geometrical rule that can solve for *all* iterative packings requires solving the following geometrical problem: Given 2 joined polyhedra, where all *intrapolyhedral* distances are known, derive a general formula for the *interpolyhedral* distances. Note that the solution to this problem immediately extends to unphysical iterative structures as well, as they are comprised of  $< n$  structures, where either (i) one or more of the joined structures is unphysical, or (ii) the particular combination of the structures is unphysical.

The geometrical problem is solved with the following observation: 2 points are fixed in 3 dimensional space if they can be related to a common triangular base. Let there exist two particles  $i, j$  whose interparticle distance,  $r_{ij}$ , is unknown. If there also exist 3 particles,  $k, p, q$ , with known interparticle distances ( $r_{kp}, r_{kq}, r_{pq}$ ), and if the distances between  $i, j$  and the 3 particle base ( $r_{ip}, r_{ik}, r_{iq}, r_{jp}, r_{jq}, r_{jq}$ ) are also known; then there exists an analytical relationship for the resulting  $r_{ij}$ , which we call the *triangular bipyramid rule*.

**4.2. Derivation of Triangular Bipyramid Rule.** We derive this rule as follows: In 3 dimensions, let the distance,  $r_{ij}$ , between 2 points,  $i$  and  $j$ , be unknown.  $i$  and  $j$  share a common 3 particle base,  $p, k, q$ . The 5 points  $i, j, k, p, q$  together form a (potentially irregular) ditetrahedron or triangular bipyramid (see figure 12). This triangular bipyramid can be decomposed into 3 related tetrahedra (see figure 13). Let us first derive a formula that relates dihedral angles ( $A_i, B_i, C_i$ ) to angles ( $a_i, b_i, c_i$ ).

Consider the general (potentially irregular) tetrahedron depicted in figure 14. The dihedral angle,  $A$ , between planes  $AOB$  and  $AOC$  can be calculated using the dot product of the normals to the planes. The normals to the planes are given by the cross products of the vectors to the vertices. Thus, this dot product is given by

$$\begin{aligned} (OA \times OB) \cdot (OA \times OC) &= (|OA||OB| \sin c)(|OA||OC| \sin b) \cos A \\ (9) \qquad \qquad \qquad &= |OA|^2 |OB||OC| \sin c \sin b \cos A. \end{aligned}$$

Using a well known vector identity, we also know that

$$\begin{aligned} (OA \times OB) \cdot (OA \times OC) &= OA \cdot [OB \times (OA \times OC)] \\ &= OA \cdot [OA(OB \cdot OC) - OC(OA \cdot OB)] \\ &= (OB \cdot OC) - (OA \cdot OC)(OA \cdot OB) \\ &= |OB||OC| \cos a - |OA||OC| \cos b |OA||OB| \cos c \\ (10) \qquad \qquad \qquad &= |OB||OC| \cos a - |OA|^2 |OC||OB| \cos b \cos c \end{aligned}$$

Setting eqn 9 = eqn 10, we thus have

$$|OA|^2 |OB||OC| \sin c \sin b \cos A = |OB||OC| \cos a - |OA|^2 |OC||OB| \cos b \cos c$$

<sup>10</sup>An iterative  $\mathcal{A}$  is an  $n \times n$  graph comprised *solely* of  $m \times m$  ( $m < n$ ) subgraphs, each of which correspond to minimally rigid  $\mathcal{A}$ 's of  $< n$  spheres.

<sup>11</sup>Given the minimal rigidity constraints we have imposed, this common base will always consist of  $\geq 3$  particles.

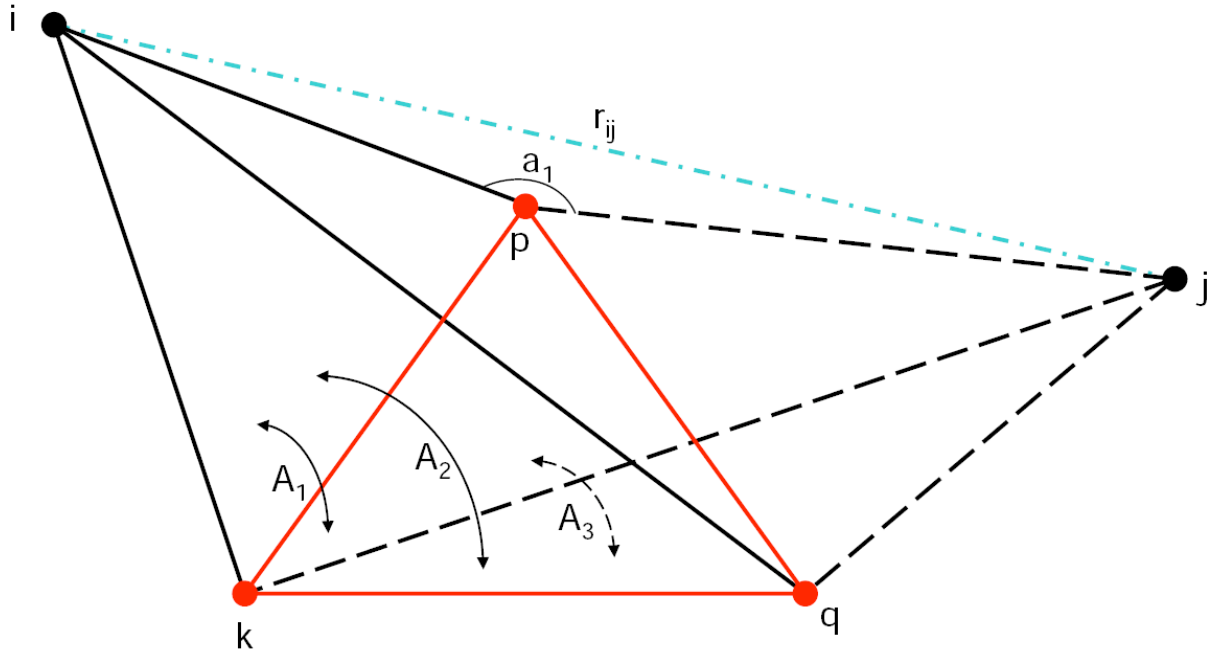


FIGURE 12. **The Triangular Bipyramid.**

The triangular bipyramid (or ditetrahedron) constructed in the triangular bipyramid rule. The center triangle ( $kpq$ ), shown in red, corresponds to the common 3 particle base. Particles  $i$  and  $j$  are related to one another through the common base. The distance between  $i$  and  $j$ ,  $r_{ij}$ , shown as the dash-dot blue line, is unknown.  $a_1$  corresponds to  $\angle jpi$ .  $A_1$  is the dihedral angle between  $\triangle ipk$  and  $\triangle jpk$ ,  $A_2$  is the dihedral angle between  $\triangle ipk$  and  $\triangle kpq$ , and  $A_3$  is the dihedral angle between  $\triangle kpq$  and  $\triangle jpk$ . Points  $i$  and  $j$  can either both lie on the same side of the base  $kpq$  or each lie on opposite sides of the base (indicated by the dashed lines, that can either go into or come out of the plane). If  $i, j$  lie on the same side, then  $A_1$  is equal to the difference of  $A_2$  and  $A_3$ , and if  $i, j$  lie on opposite sides of the base then  $A_1$  is equal to the sum of  $A_2$  and  $A_3$ . When all distances other than  $r_{ij}$  are known, then an analytical formula can be derived to solve  $r_{ij}$ .

We can divide by  $|OB|$  and  $|OC|$ , leaving us with

$$|OA|^2 \sin c \sin b \cos A = \cos a - |OA|^2 \cos b \cos c$$

and without loss of generality, we can always rescale things so that  $|OA| = 1$ , leaving us with

$$(11) \quad \sin c \sin b \cos A = \cos a - \cos b \cos c$$

Note that this formula is simply the *spherical rule of cosines*; however, in this derivation we do not assume that all radial distances are equal, as is customary in the derivation of the spherical rule of cosines. This can analogously be derived for dihedral angles  $B$  and  $C$ , in which case we obtain

$$(12) \quad \sin c \sin a \cos B = \cos b - \cos a \cos c$$

$$(13) \quad \sin a \sin b \cos C = \cos c - \cos a \cos b$$



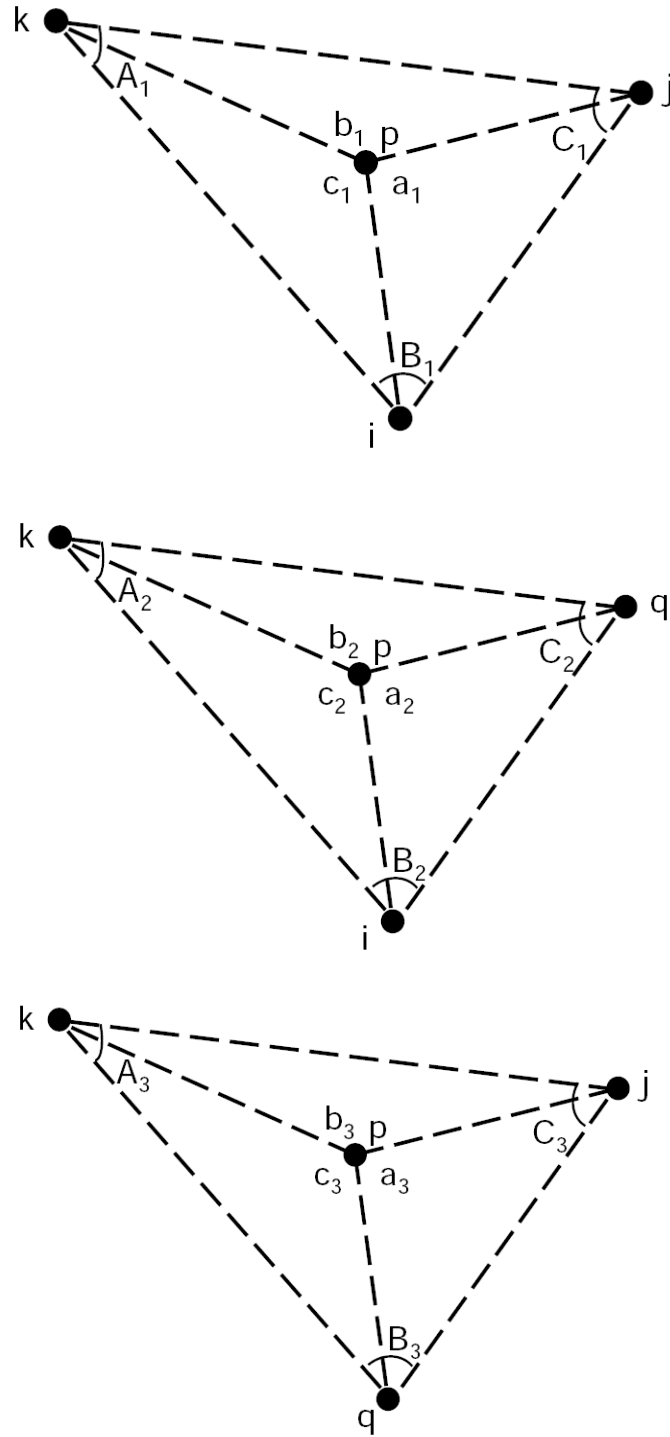


FIGURE 13. **The Tetrahedra for the Triangular Bipyramid Rule.** The 3 tetrahedra constructed for the triangular bipyramid rule. When applied to iterative packings, all of the sides of the tetrahedra are known except for side  $ij$  (corresponding to the distance  $r_{ij}$ ). The known distances can be used to calculate  $A_2$  and  $A_3$ , which in turn allows us to calculate  $A_1$ , and thus to solve for  $r_{ij}$ .

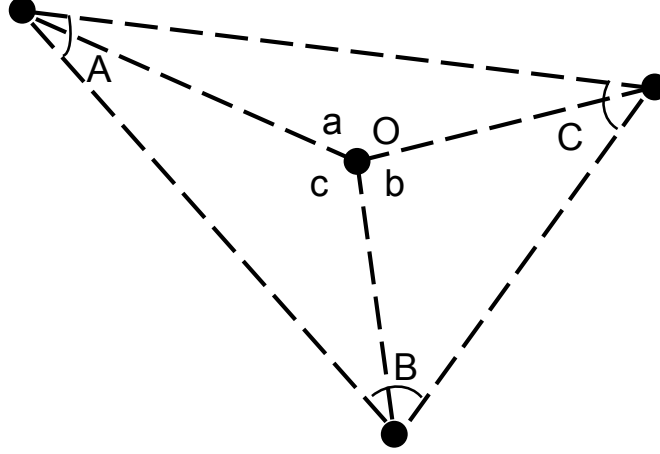


FIGURE 14. **A General Tetrahedron.**

$A, B, C$  and  $O$  label the points of the tetrahedron.  $A$  is also used to correspond to the dihedral angle between  $\triangle AOB$  and  $\triangle AOC$ ,  $B$  corresponds to the dihedral angle between  $\triangle AOB$  and  $\triangle BOC$ , and  $C$  corresponds to the dihedral angle between  $\triangle BOC$  and  $\triangle AOC$ .  $a$  corresponds to  $\angle COA$ ,  $b$  to  $\angle COB$ , and  $c$  to  $\angle AOB$ .

To derive the general formula for  $r_{ij}$ , we begin with the 3rd tetrahedron of Fig. 13 (that with angles  $A_3, B_3, a_3, b_3$ , etc.) and write down the expression for  $A_3$  using eqn 11:

$$A_3 = \cos^{-1} \left( \frac{\cos a_3 - \cos b_3 \cos c_3}{\sin c_3 \sin b_3} \right)$$

Analogously, for the 2nd tetrahedron, we have

$$A_2 = \cos^{-1} \left( \frac{\cos a_2 - \cos b_2 \cos c_2}{\sin c_2 \sin b_2} \right)$$

$A_1$  will be either the sum or the difference of the dihedral angles  $A_1$  and  $A_2$  (see fig 12), depending on whether the points  $i, j$  lie on the same or on opposite sides of the base  $p, k, q$  (on the same side,  $A_1$  corresponds to the difference, and on opposite sides to the sum).

$a_1$  is then given by

$$(14) \quad a_1 = \cos^{-1}(\sin c_1 \sin b_1 \cos A_1 + \cos b_1 \cos c_1)$$

and finally, from the law of cosines, we can calculate  $r_{ij}$ :

$$(15) \quad r_{ij} = \sqrt{r_{ip}^2 + r_{pj}^2 - 2r_{ip}r_{pj} \cos a_1}$$

Associated with each  $r_{ij}$  we have 2 possible  $A_1$ , and thus 2 possible solutions (similar, in principle, to one having 2 possible solutions to a quadratic equation).

**4.3. Applying the triangular bipyramid rule.** The triangular bipyramid rule can be used to solve all iterative packings as follows. We first search for subgraphs of  $\mathcal{A}$  corresponding to lower- $n$  seeds. The elements of  $\mathcal{D}$  corresponding to these lower order structures are known and inserted appropriately. If  $\mathcal{A}$  is iterative, all minimally rigid subgraphs of  $m < n$  particles (i.e.  $m$  subgraphs with  $\geq 3m - 6$  contacts and  $\geq 3$  contacts per particle) will correspond to  $m$  particle packings. Once all lower order seeds are inserted as appropriate, all unknown  $r_{ij}$  correspond to the distances between the spheres of different known lower order subpackings. The triangular bipyramid rule

is then applied to each unknown element<sup>12</sup> of  $\mathcal{D}$ . For each unknown distance,  $r_{ij}$ , both solutions are potentially stored, as are all possible sets of unknown distances  $\{r_{ij}\}$ . Along the way, each  $r_{ij}$  solution is tested for consistency, and it is always possible that both, 1, or neither solution will be consistent. Once all locally consistent  $r_{ij}$  are stored, the resultant  $\{r_{ij}\}$  are tested for global consistency.

A solution will be inconsistent, and thus unphysical, for one of the following reasons

1. It violates the triangle inequality (meaning that no real solution exists – this shows up as the absolute value of the argument of the inverse cosine being  $> 1$ ).
2. One or more distance(s) are  $< R$ .
3. Different triangular bases lead to different  $r_{ij}$ ; this indicates that a structure is in conflict with itself. One part of it implies it should have one structure, whereas another part implies a different structure. Such a structure is physically and mathematically inconsistent.

Violation 2 arises within the 5 particles of a singular triangular bipyramid, and thus registers a physical local inconsistency. Violation 1 occurs within individual triangular bipyramids, as each  $r_{ij}$  is solved, in which case it registers a local inconsistency; as well as over the entire set of triangular bipyramids, once all  $\{r_{ij}\}$  have been solved, in which case it registers a global inconsistency<sup>13</sup>. Violation 3 occurs when solutions are consistent within individual triangular bipyramids, and thus locally consistent, but inconsistent within combinations of triangular bipyramids – these solutions are thus *globally inconsistent*. This violation can be checked as follows: Figures 12 and 13 show that the dihedral angle,  $A_1$ , is given by either the sum or the difference of  $A_2$  and  $A_3$ , if particles  $i$  and  $j$  lie on opposite sides or on the same side of the triangular base, respectively (to within a  $2\pi$  modulation of course). Test all possible 5 particle combinations of triangular bipyramids within the  $n$  particle structure, and if there exists a triangular bipyramid that does not satisfy

$$A_1 = \begin{cases} A_2 + A_3 \\ |A_2 - A_3| \\ 2\pi - (A_2 + A_3) \\ 2\pi - |A_2 - A_3| \end{cases}$$

the solution is globally inconsistent. (In calculating  $r_{ij}$  in equation 15, we need not consider the latter two  $A_1$  solutions as  $\cos(2\pi - x) = \cos(x)$ ).

**4.4. The Growth of New Seeds.** For new seeds, we have a structure that contains an inherently new polyhedra, and thus some or all *intrapolyhedral* distances are also unknown, i.e. one or more of the 9 distances within  $\{r_{ip}, r_{ik}, r_{iq}, r_{jp}, r_{jk}, r_{jq}, r_{pk}, r_{pq}, r_{kq}\}$  are unknown. Thus, deriving the equation for  $r_{ij}$ , as is done for iterative packings, will yield one equation with  $> 1$  unknowns. The triangular bipyramid rule, therefore, can not be applied directly to new seeds, and new geometrical rules must be derived to analytically solve non-iterative  $\mathcal{A}$ 's.

Using a general rule to solve for iterative  $\mathcal{A}$ 's, and deriving individual geometrical rules for non-iterative  $\mathcal{A}$ 's is feasible so long as the non-iterative  $\mathcal{A}$ 's do not grow too quickly with  $n$ .

<sup>12</sup>If  $\mathcal{A}$  is not iterative, there will exist unknown  $r_{ij}$  that do not correspond to distances between spheres of known subpackings. In this case, eqn 15 will contain  $\geq 1$  unknown element on the right hand side and can not be applied directly.

<sup>13</sup>In this case, some triangular bipyramids are locally consistent, whereas others are not. All possible triangular bipyramids of a structure need not be tested to solve for all  $r_{ij}$ , thus it is important to check all bipyramids to ensure global consistency once  $\{r_{ij}\}$  have been solved. This violation is related to violation 3, except that here the violation is registered between the angles associated with the line segments, and in violation 3 the violation occurs within the dihedral angles.

Table 1 shows that this is the case for  $n \leq 9$ , where the number of non-iterative  $\mathcal{A}$ 's is  $\leq 5$ . However, at  $n = 10$ , there are 126 non-iterative  $\mathcal{A}$ 's<sup>14</sup>. To sift through the 126 potential seeds at  $n=10$  requires inventing new geometrical rules, and the growth of such rules demonstrates that the method we have described does not scale efficiently with  $n$ . In section 7.2, we will discuss a potential extension of the triangular bipyramid rule, which might be able to break this bottleneck, at least computationally. Here, we present the packing results derived from a combination of the triangular bipyramid rule applied to iterative  $\mathcal{A}$ 's, and individual geometrical rules applied to non-iterative  $\mathcal{A}$ 's<sup>15</sup>. For  $n \leq 9$ , we have analytically solved for all packings. At  $n = 10$ , we analytically solve for all iterative packings, and produce a preliminary list of new seeds, found by constructing the non-iterative  $\mathcal{A}$ 's manually with the construction toy *Geomags*.

## 5. THE SET OF SPHERE PACKINGS

Here we present the list of sphere packings derived by this method. In principle, the analytical method outlined here will yield a provably complete set of packings. However, we have not implemented the triangular bipyramid rule symbolically, leading to the following practical issues, which could lead to numerical errors:

*Numerical round-off error:* All calculations involving the triangular bipyramid rule are subject to numerical precision. This means that we can encounter situations in which the  $\cos^{-1}$  term used to solve the angles and dihedral angles of a packing (such as in eqn 14) can show up as  $\cos^{-1}(1+\varepsilon)$ , where  $\varepsilon$  is the numerical round-off error. As  $\cos^{-1}(1+\varepsilon)$  is undefined, this can cause packings to erroneously be recognized as unphysical<sup>16</sup>. Similarly, in checking for the equivalence between dihedral angles when checking for the consistency of a packing, equality checking must be done modulo round off error. Round off issues could be improved by using general precision libraries such as gmp and mpfr [1, 2], or altogether avoided by doing all calculations symbolically. Thus, while the analytical method presented here should in principle yield a provably complete set of sphere packings, practical issues such as these are a potential source of error.

We present a complete set of sphere packings of  $n \leq 9$ , save round-off error. At  $n = 10$ , we present a complete set of iterative packings and a preliminary list of new seeds. Packings of  $n \leq 7$  particles are included here, and packings of  $n \leq 8 \leq 10$  particles are included in supplementary information [8].

In the list presented here,  $\phi$  corresponds to the point group, and  $\sigma$  to the symmetry number. We have included the 2nd moment of each packing, and a ‘\*’ appears next to the 2nd moment that corresponds to the minimum of the 2nd moment of  $n$  particles. The ‘special properties’ column denotes whether a structure is convex, a new seed, chiral, or non-rigid. If the special properties column is blank, then that packing contains none of these properties.

---

<sup>14</sup>Note that the non-iterative and iterative  $\mathcal{A}$ 's listed in this table are constructed *after* applying the geometrical rules for  $n \leq 8$  that appear in the text and in the supplementary information [8]. Thus, this reflects the number of iterative and non-iterative  $\mathcal{A}$ 's with respect to these geometrical rules, and not the absolute number of iterative and non-iterative  $\mathcal{A}$ 's

<sup>15</sup>Because of the chronological order in which these rules were derived, the code implements individual geometrical rules for all packings of  $\leq 6$  particles, and begins applying the triangular bipyramid rule for  $n \geq 7$  – thus some iterative structures and sub-structures are solved using individual geometrical rules.

<sup>16</sup>Note that a legitimate way of determining that a packing is mathematically inconsistent, and thus not physically possible, is encountering the situation  $\cos^{-1}(a)$ , where  $|a| > 1$ , which is why this round-off error is a legitimate source of error.

## 2 Particle Packings

Packing 1 (Graph 1):

$$\begin{aligned} \mathcal{A} &: \begin{pmatrix} 0 & 1 \\ 1 & 0 \end{pmatrix} \\ \mathcal{D} &: \begin{pmatrix} 0 & 1 \\ 1 & 0 \end{pmatrix} R \\ \mathcal{C} &: \begin{pmatrix} 0 \\ 0 \\ 0 \\ 0 \\ -1 \\ 0 \end{pmatrix} R \end{aligned}$$

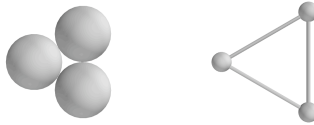


2nd Moment	$\phi$	$\sigma$	Special Properties
$*0.5R^2$	$D_{\infty h}$	2	New Seed Convex

## 3 Particle Packings

Packing 1 (Graph 1):

$$\begin{aligned} \mathcal{A} &: \begin{pmatrix} 0 & 1 & 1 \\ 1 & 0 & 1 \\ 1 & 1 & 0 \end{pmatrix} \\ \mathcal{D} &: \begin{pmatrix} 0 & 1 & 1 \\ 1 & 0 & 1 \\ 1 & 1 & 0 \end{pmatrix} R \\ \mathcal{C} &: \begin{pmatrix} 0 \\ 0 \\ 0 \\ 0 \\ -1 \\ 0 \\ \sqrt{3}/2 \\ -1/2 \\ 0 \end{pmatrix} R \end{aligned}$$



2nd Moment	$\phi$	$\sigma$	Special Properties
$*1.0R^2$	$D_{3h}$	6	Convex

#### 4 Particle Packings

Packing 1 (Graph 1):

$$\mathcal{A}: \begin{pmatrix} 0 & 1 & 1 & 1 \\ 1 & 0 & 1 & 1 \\ 1 & 1 & 0 & 1 \\ 1 & 1 & 1 & 0 \end{pmatrix}$$

$$\mathcal{D}: \begin{pmatrix} 0 & 1 & 1 & 1 \\ 1 & 0 & 1 & 1 \\ 1 & 1 & 0 & 1 \\ 1 & 1 & 1 & 0 \end{pmatrix} R$$

$$\mathcal{C}: \begin{pmatrix} 0 \\ 0 \\ 0 \\ 0 \\ -1 \\ 0 \\ \sqrt{3}/2 \\ -1/2 \\ 0 \\ 1/(2\sqrt{3}) \\ -1/2 \\ \sqrt{2/3} \end{pmatrix} R$$



2nd Moment	$\phi$	$\sigma$	Special Properties
$*1.5R^2$	$T_d$	12	Convex

#### 5 Particle Packings

Packing 1 (Graph 1):

$$\mathcal{A}: \begin{pmatrix} 0 & 0 & 1 & 1 & 1 \\ 0 & 0 & 1 & 1 & 1 \\ 1 & 1 & 0 & 1 & 1 \\ 1 & 1 & 1 & 0 & 1 \\ 1 & 1 & 1 & 1 & 0 \end{pmatrix}$$

$$\mathcal{D}: \begin{pmatrix} 0 & 2\sqrt{\frac{2}{3}} & 1 & 1 & 1 \\ 2\sqrt{\frac{2}{3}} & 0 & 1 & 1 & 1 \\ 1 & 1 & 0 & 1 & 1 \\ 1 & 1 & 1 & 0 & 1 \\ 1 & 1 & 1 & 1 & 0 \end{pmatrix} R$$

$$\mathcal{C}: \begin{pmatrix} 0 \\ 0 \\ 0 \\ 4/(3\sqrt{3}) \\ -4/3 \\ (2/3)\sqrt{2/3} \\ 1/(2\sqrt{3}) \\ -1/2 \\ \sqrt{2/3} \\ 0 \\ -1 \\ 0 \\ \sqrt{3}/2 \\ -1/2 \\ 0 \end{pmatrix} R$$



2nd Moment	$\phi$	$\sigma$	Special Properties
$*2.33333R^2$	$D_{3h}$	6	Convex

## 6 Particle Packings

Packing 1 (Graph 2):

$$\mathcal{A}: \begin{pmatrix} 0 & 0 & 1 & 1 & 1 & 1 \\ 0 & 0 & 0 & 1 & 1 & 1 \\ 1 & 0 & 0 & 0 & 1 & 1 \\ 1 & 1 & 0 & 0 & 1 & 1 \\ 1 & 1 & 1 & 1 & 0 & 1 \\ 1 & 1 & 1 & 1 & 1 & 0 \end{pmatrix}$$

$$\mathcal{D}: \begin{pmatrix} 0 & 2\sqrt{\frac{2}{3}} & 1 & 1 & 1 & 1 \\ 2\sqrt{\frac{2}{3}} & 0 & \frac{5}{3} & 1 & 1 & 1 \\ 1 & \frac{5}{3} & 0 & 2\sqrt{\frac{2}{3}} & 1 & 1 \\ 1 & 1 & 2\sqrt{\frac{2}{3}} & 0 & 1 & 1 \\ 1 & 1 & 1 & 1 & 0 & 1 \\ 1 & 1 & 1 & 1 & 1 & 0 \end{pmatrix} R$$

$$\mathcal{C}: \begin{pmatrix} 4/(3\sqrt{3}) \\ 1/3 \\ (2/3)\sqrt{2/3} \\ 0 \\ -1 \\ 0 \\ 20/(9\sqrt{3}) \\ -4/9 \\ (10/9)\sqrt{2/3} \\ 0 \\ 0 \\ 0 \\ 1/(2\sqrt{3}) \\ -1/2 \\ \sqrt{2/3} \\ \sqrt{3}/2 \\ -1/2 \\ 0 \end{pmatrix} R$$



2nd Moment	$\phi$	$\sigma$	Special Properties
$3.35185R^2$	$C_{2v}$	2	

Packing 2 (Graph 4):

$$\mathcal{A}: \begin{pmatrix} 0 & 0 & 1 & 1 & 1 & 1 \\ 0 & 0 & 1 & 1 & 1 & 1 \\ 1 & 1 & 0 & 0 & 1 & 1 \\ 1 & 1 & 0 & 0 & 1 & 1 \\ 1 & 1 & 1 & 1 & 0 & 0 \\ 1 & 1 & 1 & 1 & 0 & 0 \end{pmatrix}$$

$$\mathcal{D}: \begin{pmatrix} 0 & \sqrt{2} & 1 & 1 & 1 & 1 \\ \sqrt{2} & 0 & 1 & 1 & 1 & 1 \\ 1 & 1 & 0 & \sqrt{2} & 1 & 1 \\ 1 & 1 & \sqrt{2} & 0 & 1 & 1 \\ 1 & 1 & 1 & 1 & 0 & \sqrt{2} \\ 1 & 1 & 1 & 1 & \sqrt{2} & 0 \end{pmatrix} R$$

$$\mathcal{C}: \begin{pmatrix} 0 \\ 0 \\ 0 \\ 1 \\ -1 \\ 0 \\ 0 \\ -1 \\ 0 \\ 1 \\ 0 \\ 0 \\ 1/2 \\ -1/2 \\ \sqrt{2}/2 \\ 1/2 \\ -1/2 \\ -\sqrt{2}/2 \end{pmatrix} R$$



2nd Moment	$\phi$	$\sigma$	Special Properties
$*3.0R^2$	$O_h$	24	New Seed Convex

## 7 Particle Packings

Packing 1 (Graph 4):

$$\mathcal{A} : \begin{pmatrix} 0 & 0 & 0 & 1 & 1 & 1 & 1 \\ 0 & 0 & 0 & 1 & 0 & 1 & 1 \\ 0 & 0 & 0 & 0 & 1 & 1 & 1 \\ 1 & 1 & 0 & 0 & 0 & 1 & 1 \\ 1 & 0 & 1 & 0 & 0 & 1 & 1 \\ 1 & 1 & 1 & 1 & 1 & 0 & 1 \\ 1 & 1 & 1 & 1 & 1 & 1 & 0 \end{pmatrix}$$

$$\mathcal{D} : \begin{pmatrix} 0 & 2\sqrt{\frac{2}{3}} & 2\sqrt{\frac{2}{3}} & 1 & 1 & 1 & 1 \\ 2\sqrt{\frac{2}{3}} & 0 & 4\sqrt{\frac{6}{9}} & 1 & \frac{5}{3} & 1 & 1 \\ 2\sqrt{\frac{2}{3}} & 4\sqrt{\frac{6}{9}} & 0 & \frac{5}{3} & 1 & 1 & 1 \\ 1 & 1 & \frac{5}{3} & 0 & 2\sqrt{\frac{2}{3}} & 1 & 1 \\ 1 & \frac{5}{3} & 1 & 2\sqrt{\frac{2}{3}} & 0 & 1 & 1 \\ 1 & 1 & 1 & 1 & 1 & 0 & 1 \\ 1 & 1 & 1 & 1 & 1 & 1 & 0 \end{pmatrix} R$$

$$\mathcal{C} : \begin{pmatrix} 0 \\ 0 \\ 0 \\ 4/(3\sqrt{3}) \\ -4/3 \\ (2/3)\sqrt{2/3} \\ 20/(9\sqrt{3}) \\ -4/9 \\ (10/9)\sqrt{2/3} \\ 0 \\ -1 \\ 0 \\ 4\sqrt{3}/9 \\ 1/3 \\ (2/3)\sqrt{2/3} \\ \sqrt{3}/2 \\ -1/2 \\ 0 \\ 1/(2\sqrt{3}) \\ -1/2 \\ \sqrt{2/3} \end{pmatrix} R$$



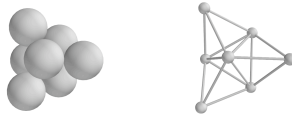
2nd Moment	$\phi$	$\sigma$	Special Properties
$4.24868R^2$	$C_{2v}$	2	

Packing 2 (Graph 8):

$$\mathcal{A} : \begin{pmatrix} 0 & 0 & 0 & 1 & 1 & 0 & 1 \\ 0 & 0 & 0 & 1 & 0 & 1 & 1 \\ 0 & 0 & 0 & 0 & 1 & 1 & 1 \\ 1 & 1 & 0 & 0 & 1 & 1 & 1 \\ 1 & 0 & 1 & 1 & 0 & 1 & 1 \\ 0 & 1 & 1 & 1 & 1 & 0 & 1 \\ 1 & 1 & 1 & 1 & 1 & 1 & 0 \end{pmatrix}$$

$$\mathcal{D} : \begin{pmatrix} 0 & \frac{5}{3} & \frac{5}{3} & 1 & 1 & 2\sqrt{\frac{2}{3}} & 1 \\ \frac{5}{3} & 0 & \frac{5}{3} & 1 & 2\sqrt{\frac{2}{3}} & 1 & 1 \\ \frac{5}{3} & \frac{5}{3} & 0 & 2\sqrt{\frac{2}{3}} & 1 & 1 & 1 \\ 1 & 1 & 2\sqrt{\frac{2}{3}} & 0 & 1 & 1 & 1 \\ 1 & 2\sqrt{\frac{2}{3}} & 1 & 1 & 0 & 1 & 1 \\ 2\sqrt{\frac{2}{3}} & 1 & 1 & 1 & 1 & 0 & 1 \\ 1 & 1 & 1 & 1 & 1 & 1 & 0 \end{pmatrix} R$$

$$\mathcal{C} : \begin{pmatrix} 0 \\ -1 \\ 0 \\ -5/(18\sqrt{3}) \\ 7/18 \\ (10/9)\sqrt{2/3} \\ 20/(9\sqrt{3}) \\ -4/9 \\ (10/9)\sqrt{2/3} \\ 0 \\ 0 \\ 0 \\ \sqrt{3}/2 \\ -1/2 \\ 0 \\ 4\sqrt{3}/9 \\ 1/3 \\ (2/3)\sqrt{2/3} \\ 1/(2\sqrt{3}) \\ -1/2 \\ \sqrt{2/3} \end{pmatrix} R$$



2nd Moment	$\phi$	$\sigma$	Special Properties
$4.47619R^2$	$C_{3v}$	3	

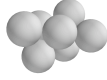


Packing 3 (Graph 17):

$$\mathcal{A}: \begin{pmatrix} 0 & 0 & 1 & 0 & 1 & 1 & 1 \\ 0 & 0 & 0 & 1 & 1 & 1 & 1 \\ 1 & 0 & 0 & 0 & 1 & 0 & 1 \\ 0 & 1 & 0 & 0 & 0 & 1 & 1 \\ 1 & 1 & 1 & 0 & 0 & 1 & 1 \\ 1 & 1 & 0 & 1 & 1 & 0 & 1 \\ 1 & 1 & 1 & 1 & 1 & 1 & 0 \end{pmatrix}$$

$$\mathcal{D}: \begin{pmatrix} 0 & 2\sqrt{\frac{2}{3}} & 1 & \frac{5}{3} & 1 & 1 & 1 \\ 2\sqrt{\frac{2}{3}} & 0 & \frac{5}{3} & 1 & 1 & 1 & 1 \\ 1 & \frac{5}{3} & 0 & \frac{1}{3}\sqrt{\frac{107}{3}} & 1 & 2\sqrt{\frac{2}{3}} & 1 \\ \frac{5}{3} & 1 & \frac{1}{3}\sqrt{\frac{107}{3}} & 0 & 2\sqrt{\frac{2}{3}} & 1 & 1 \\ 1 & 1 & 1 & 2\sqrt{\frac{2}{3}} & 0 & 1 & 1 \\ 1 & 1 & 2\sqrt{\frac{2}{3}} & 1 & 1 & 0 & 1 \\ 1 & 1 & 1 & 1 & 1 & 1 & 0 \end{pmatrix} R$$

$$C: \begin{pmatrix} 4\sqrt{3}/9 \\ 1/3 \\ (2/3)\sqrt{2/3} \\ 0 \\ -1 \\ 0 \\ 20/(9\sqrt{3}) \\ -4/9 \\ (10/9)\sqrt{2/3} \\ -7/(6\sqrt{3}) \\ -1/2 \\ (2/3)\sqrt{2/3} \\ \sqrt{3}/2 \\ -1/2 \\ 0 \\ 0 \\ 0 \\ 0 \\ 1/(2\sqrt{3}) \\ -1/2 \\ \sqrt{2/3} \end{pmatrix} R$$



2nd Moment	$\phi$	$\sigma$	Special Properties
$4.64550R^2$	$C_2$	2	Chiral

Packing 4 (Graph 22):

$$\mathcal{A}: \begin{pmatrix} 0 & 0 & 1 & 1 & 0 & 1 & 1 \\ 0 & 0 & 0 & 1 & 1 & 1 & 1 \\ 1 & 0 & 0 & 0 & 1 & 1 & 1 \\ 1 & 1 & 0 & 0 & 0 & 1 & 1 \\ 0 & 1 & 1 & 0 & 0 & 1 & 1 \\ 1 & 1 & 1 & 1 & 1 & 0 & 0 \\ 1 & 1 & 1 & 1 & 1 & 0 & 0 \end{pmatrix}$$

$$\mathcal{D}: \begin{pmatrix} 0 & \sqrt{\frac{3+\sqrt{5}}{2}} & 1 & 1 & \sqrt{\frac{3+\sqrt{5}}{2}} & 1 & 1 \\ \sqrt{\frac{3+\sqrt{5}}{2}} & 0 & \sqrt{\frac{3+\sqrt{5}}{2}} & 1 & 1 & 1 & 1 \\ 1 & \sqrt{\frac{3+\sqrt{5}}{2}} & 0 & \sqrt{\frac{3+\sqrt{5}}{2}} & 1 & 1 & 1 \\ 1 & 1 & \sqrt{\frac{3+\sqrt{5}}{2}} & 0 & \sqrt{\frac{3+\sqrt{5}}{2}} & 1 & 1 \\ \sqrt{\frac{3+\sqrt{5}}{2}} & 1 & 1 & \sqrt{\frac{3+\sqrt{5}}{2}} & 0 & 1 & 1 \\ 1 & 1 & 1 & 1 & 1 & 0 & \sqrt{2-\frac{2}{\sqrt{5}}} \\ 1 & 1 & 1 & 1 & 1 & \sqrt{2-\frac{2}{\sqrt{5}}} & 0 \end{pmatrix} R$$

$$C: \begin{pmatrix} 0 \\ 0 \\ 0 \\ (1/2)\sqrt{(1/2)(5+\sqrt{5})} \\ (1/4)(-3-\sqrt{5}) \\ 0 \\ (1/2)\sqrt{(1/2)(5+\sqrt{5})} \\ (1/4)(-1-\sqrt{5}) \\ 0 \\ 0 \\ -1 \\ 0 \\ (1/8)(\sqrt{2(5+\sqrt{5})} + \sqrt{10(5+\sqrt{5})}) \\ -1/2 \\ 0 \\ (5+\sqrt{5})^{3/2}/(20\sqrt{2}) \\ -1/2 \\ \sqrt{(1/10)(5-\sqrt{5})} \\ (5+\sqrt{5})^{3/2}/(20\sqrt{2}) \\ -1/2 \\ -\sqrt{(1/10)(5-\sqrt{5})} \end{pmatrix} R$$



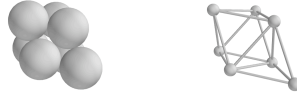
2nd Moment	$\phi$	$\sigma$	Special Properties
*4.17082R <sup>2</sup>	$D_{5h}$	10	New Seed Convex

Packing 5 (Graph 26):

$$\mathcal{A} : \begin{pmatrix} 0 & 0 & 1 & 1 & 1 & 1 & 1 \\ 0 & 0 & 0 & 1 & 1 & 1 & 1 \\ 1 & 0 & 0 & 0 & 1 & 0 & 1 \\ 1 & 1 & 0 & 0 & 0 & 1 & 1 \\ 1 & 1 & 1 & 0 & 0 & 1 & 1 \\ 1 & 1 & 0 & 1 & 1 & 0 & 0 \\ 1 & 1 & 1 & 1 & 1 & 0 & 0 \end{pmatrix}$$

$$\mathcal{D} : \begin{pmatrix} 0 & \sqrt{2} & 1 & 1 & 1 & 1 & 1 \\ \sqrt{2} & 0 & \sqrt{3} & 1 & 1 & 1 & 1 \\ 1 & \sqrt{3} & 0 & \sqrt{3} & 1 & \sqrt{3} & 1 \\ 1 & 1 & \sqrt{3} & 0 & \sqrt{2} & 1 & 1 \\ 1 & 1 & 1 & \sqrt{2} & 0 & 1 & 1 \\ 1 & 1 & \sqrt{3} & 1 & 1 & 0 & \sqrt{2} \\ 1 & 1 & 1 & 1 & 1 & \sqrt{2} & 0 \end{pmatrix} R$$

$$\mathcal{C} : \begin{pmatrix} 1 \\ -1 \\ 0 \\ 0 \\ 0 \\ 3/2 \\ -1/2 \\ \sqrt{2}/2 \\ 0 \\ -1 \\ 0 \\ 1 \\ 0 \\ 0 \\ 1/2 \\ -1/2 \\ -\sqrt{2}/2 \\ 1/2 \\ -1/2 \\ \sqrt{2}/2 \end{pmatrix} R$$



2nd Moment	$\phi$	$\sigma$	Special Properties
$4.28571R^2$	$C_{3v}$	3	Convex

## 6. PROPERTIES OF PACKINGS

Here we highlight some interesting properties of packings.

**6.1. New Seeds.** New seeds are interesting because they are inherently new structures of  $n$  particles. They are also ‘generating sets,’ i.e. once they exist at a given starting  $n = m$ , they are propagated iteratively for all  $n > m$ . Geometrically, new seeds are inherently global structures, stabilized *exactly* by the  $n$  particles for which that new seed arises. Iterative packings are geometrically locally stable, in that  $< n$  subsets of the packing also correspond to packings. Thus, new seeds are unique events for a given number of particles,  $n$ . Figure 15 shows all new seeds of  $n \leq 10$  particles (where the set of new seeds at  $n = 10$  is putative). The proportion of new seeds to total packings is relatively small for small  $n$ , which can be seen in table 4.

**6.2. Rigidity.** We have enumerated packings satisfying minimal rigidity constraints; these constraints are necessary but not sufficient for rigidity, and thus we can find non-rigid packings that satisfy these constraints. For these packings, there exists a degree of freedom in which particles can move without breaking or forming additional contacts. The first instance of a non-rigid packing occurs at  $n = 9$ , at which there is one. At  $n = 10$ , there are 4 non-rigid packings: 1 non-rigid new seed, and 3 iterative non-rigid packings that derive from the  $n = 9$  non-rigid new seed (Fig. 16 and 17).

These 10 particle non-rigid packings will iteratively produce at least  $m \geq 1$  non-rigid packings at  $n = 11$ , and so on. All non-rigid packings enumerated thus far contain  $\geq 2$  deformable open square faces. We do not know whether or not  $\geq 2$  open square faces are a requisite of non-rigid

$n$	Packings from [23]	Total Packings (Current Study)	New Seeds	Non-Rigid Packings	Chiral	Total States
2	1	1	0	0	0	1
3	1	1	0	0	0	1
4	1	1	0	0	0	1
5	1	1	0	0	0	1
6	2	2	1	0	0	2
7	4	5	1	0	1	6
8	10	13	1	0	3	16
9	32	50	4	1	27	77
10	113	223	8	4	170	393

TABLE 4. **Packings.**

Total number of packings found by the current study, compared to those found by Hoare and McInnes [23], who used only the tetrahedral ( $n = 4$ ) and octahedral ( $n = 8$ ) seeds to iteratively calculate hard sphere packings by adding one particle at a time to  $n - 1$  particle packings. They include chiral structures within their list of packings, so that a left and right-handed packing is considered to be 2 packings. We distinguish between chiral structures and packings, such that a left and right-handed packing is considered to be 1 packing with 2 distinct states (for  $n \leq 10$  this is the only type of chiral packing encountered). The number of packings having chiral counterparts is included in the column marked ‘chiral.’ The total number of states per  $n$  is equal to the number of packings plus the number of chiral structures. This is included in the table, along with the number of packings corresponding to new seeds and to non-rigid structures.

packings that satisfy minimal rigidity constraints. The open square faces must be ‘connected’ for the extra degree of freedom to exist – in the packings encountered thus far, this manifests itself by the existence of half-octahedra sharing  $\geq 1$  vertex.

**6.3. The Tree Nature of Packings.** There is a distinct tree nature to packings. New seeds are the origin of a branch in the tree. Iterative packings continue the branch. All  $n$  particle iterative packings can be decomposed into combinations of  $< n$  particle packings, and this decomposition is often not unique. When the decomposition is not unique, the branches of the tree converge. Figures 18 and 19 show examples of tree convergence. Figure 18 shows the 2 possible decompositions of one of the 10 particle 25 contact packings. This packing can be formed either by adding 1 particle to the 9 particle non-rigid new seed, or by combining two polytetrahedra with a 6 particle octahedron.

Figure 19 shows the tree structure of  $2 \leq n \leq 8$  packings. It can be seen that tree convergence occurs from  $n = 7$  to  $n = 8$ , where multiple 7 particle packings produce the same 8 particle packing under the addition of another particle.

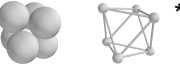
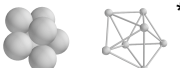

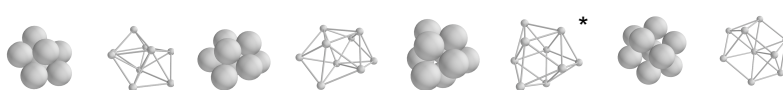
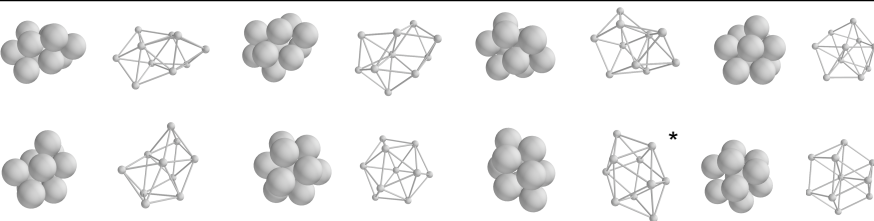
n = 6	
n = 7	
n = 8	
n = 9	
n = 10	

FIGURE 15. **New Seeds.**

All new seeds of  $n \leq 10$  particles shown in both sphere and point/line representation. There exists only 1 packing for each  $n$  of  $n \leq 5$  particles, that can each be constructed iteratively from a dimer; thus there exist no new seeds for  $n \leq 5$ .  $n = 6$  is the first instance of a new seed. The set of new seeds reported for  $n = 10$  is putative and thus represents a lower bound. New seeds with a \* appearing to the right correspond to minima of the second moment out of all packings for that  $n$ . It can be seen here that the minimum of the second moment corresponds to a seed, if one exists. As there is only one possible packing for each  $n \leq 5$ , the minimum of the 2nd moment simply corresponds to that unique packing.

**6.4. Minima of the Second Moment.** The second moment measures the deviation of particles from their collective center (centroid), and is given by

$$(16) \quad M = \sum_{i=1}^n |\mathbf{r}_i - \mathbf{c}|^2 = \sum_{i=1}^n (x_i - c_x)^2 + (y_i - c_y)^2 + (z_i - c_z)^2$$

where  $\mathbf{r}_i$  is the  $x, y, z$  position of particle  $i$ ; and  $\mathbf{c}$  is the centroid, the average  $x, y, z$  position over all particles, given by

$$(17) \quad c_x = \frac{1}{n} \sum_{i=1}^n x_i$$

and analogously given for  $c_y$  and  $c_z$ .

The minimum of the second moment corresponds to the packing with the smallest  $M$ . The 2nd moment is listed within the list of packings in section 5 and appendix B, and a “\*” signifies the minimum of the 2nd moment for each  $n$  in Fig. 15. We confirm that the minima of the 2nd moment reported by Sloane and Conway [43] are correct (they proved the 2nd moment minima

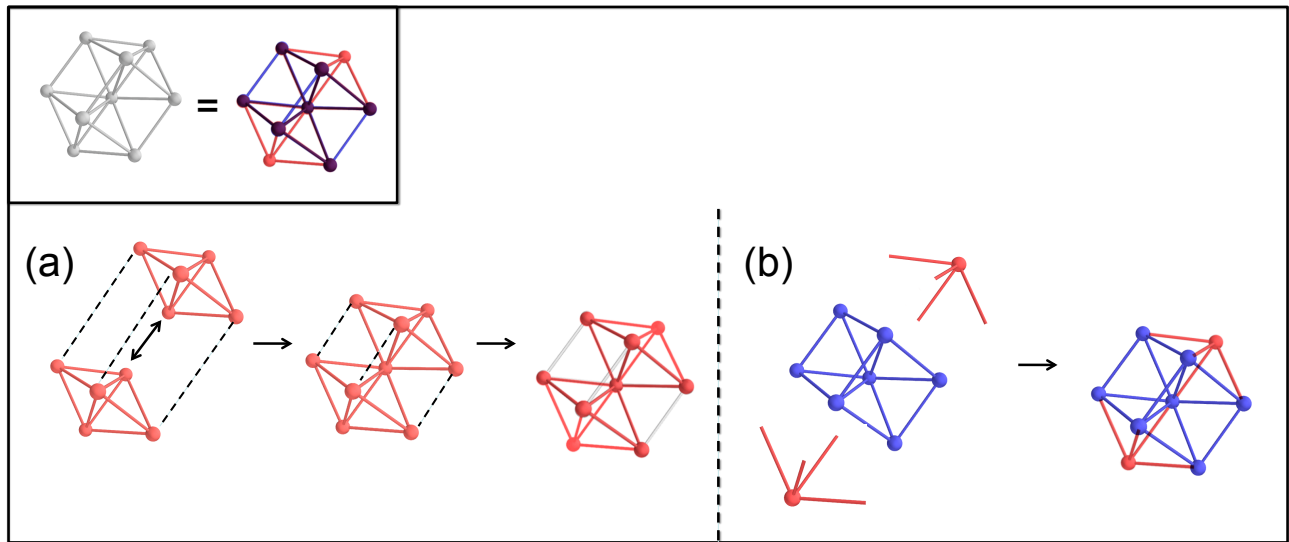


FIGURE 16. The 9 particle non-rigid new seed (grey) is shown in the top left-hand box. It is composed of two joined 5 point polytetrahedra (red) attached to two joined half octahedra (blue). The substructures are shown overlain – purple bonds and particles are shared by both substructures; whereas only red or blue bonds and particles belong to the polytetrahedral or octahedral structures alone, respectively. Two representative ways of forming this non-rigid structure are shown in (a) and (b). (a) Two 5 point poltetrahedra are joined by sharing one common point (on bottom). The two polytetrahedra are then fully attached to one another via the remaining 3 bonds first shown in dashed black lines, as potential bonds, and then in solid white lines, as actualized bonds. These bonds form the two connected half octahedra. (b) 2 particles (red) are attached to the concave side faces of the 2 joined half octahedra (blue). The 2 red particles form the two 5 point polytetrahedral substructures once they are attached to the joined octahedra.

for  $n \leq 4$ , but for  $n > 4$  these were putative structures). For  $n \leq 10$ , the minima of the second moment corresponds to a new seed, if a new seed exists.

**6.5. Ground States and the Maximum Number of Contacts.** A fundamental question related to sphere packings is what is the maximum number of contacts that a packing of  $n$  spheres can have? Not only is this question of mathematical interest in its own right, but it is also of significant physical interest as such packings correspond to ground states. The number of packings that contain the maximal number of contacts in turn corresponds to the ground state degeneracy. Fig. 20 and table 6.5 show how the ground state degeneracy changes with  $n$ . Interestingly, this relation appears to be oscillatory.

For  $n \leq 9$  every packing has exactly  $3n - 6$  contacts. As, for this system, the potential energy is linearly proportional to the number of contacts<sup>17</sup>; all packings at each  $n$ ,  $n \leq 9$ , have the same potential energy. Fig. 20 shows that, for  $n \leq 9$ , the ground state degeneracy increases exponentially. But at  $n = 10$  this trend changes due to a small number of packings that can have

<sup>17</sup>The potential energy is a pairwise additive function of the interparticle distances:  $\sum_{ij} f(r_{ij})$ , where  $f$  is any function, and  $r_{ij}$  is the distance between particles  $i$  and  $j$ .

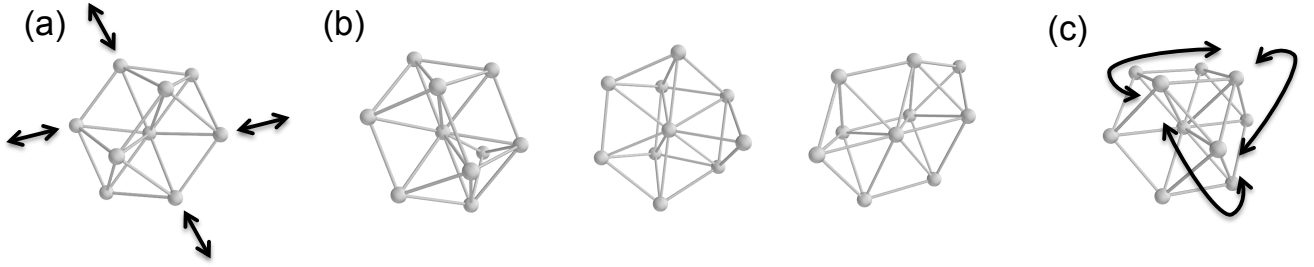


FIGURE 17. Non-rigid packings of 9 and 10 spheres. (a) The non-rigid  $n = 9$  packing, with non-rigid motion, corresponding to a twisting of the square faces, shown by black arrows. (b) Non-rigid  $n = 10$  packings formed iteratively by adding one particle to the non-rigid  $n = 9$  seed. The non-rigid motion of these structures is the same as in (a). (c) Non-rigid  $n = 10$  seed. Non-rigid motion, corresponding to a twisting of the radially connected square faces connected by the top triangle, is shown by the black arrows.

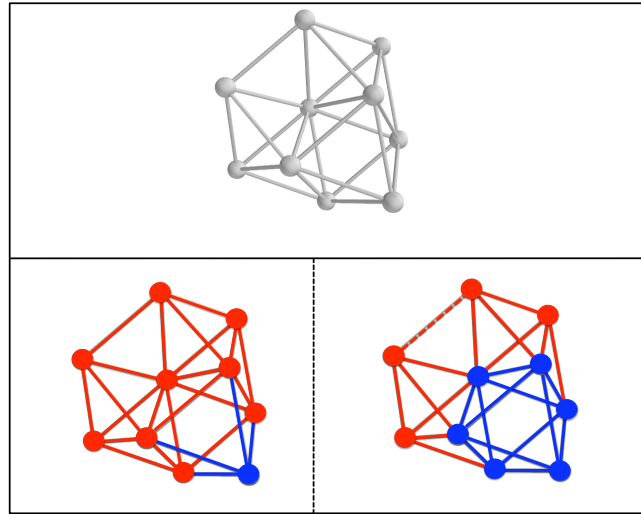


FIGURE 18. **Tree Convergence in a 10 Particle Packing.**

An example of tree convergence in one of the 25 contact packings of 10 particles. This packing, shown in grey (top panel), can be decomposed into (bottom left panel) the 9 particle non-rigid new seed (red) plus one particle (blue) that rigidifies the structure, or into (bottom right panel) an octahedron (blue) with 2 attached polytetrahedra (red). The red dashed line indicates an ‘implicit contact,’ a contact that automatically forms once the other contacts are in place (this corresponds to the 25th contact).

$25 = 3n - 5$  contacts (all other 10 particle packings have  $3n - 6$  contacts). There exist 3 such packings, each containing octahedra (Fig. 21a-c). These three structures are the ground states at  $n = 10$ .

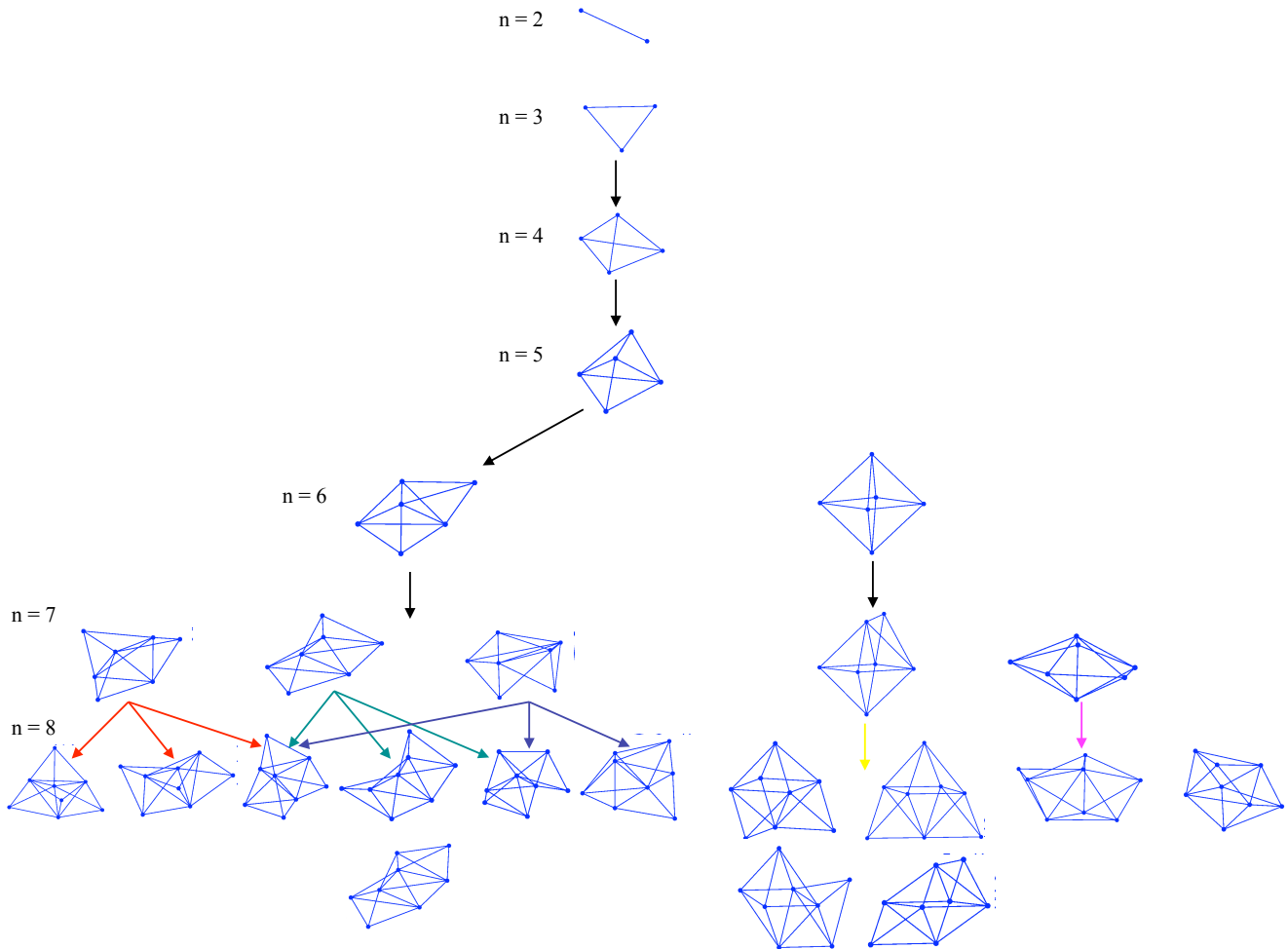


FIGURE 19. **Tree Convergence for  $n \leq 8$ .**

An example of tree convergence for  $2 \leq n \leq 8$ . Packings above which there is no arrow correspond to new seeds, and thus the beginning of a new branch. The arrows then point to the  $n$  particle packing or group of packings that form iteratively by adding one particle. It can be seen that even for the iterative case of adding one particle, there is tree convergence from  $n = 7$  to  $n = 8$  (shown by multiple arrows feeding into the same packing).

For  $n \geq 11$ , we conjecture as to what the maximal number of contacts are, and provide examples of such structures. The maximal contact packings at  $n = 10$  arise because it becomes possible to add 4 contacts to minimally rigid 9 particle packings; whereas all other iterative packings of  $n \leq 10$  spheres are formed by the addition of  $3m$  contacts to a minimally rigid  $n - m$  sphere packing. All maximal contact packings found thus far correspond to iterative packings. We have not determined whether this is true for all  $n$ , but we conjecture that it is, because new seeds tend to contain more empty space, and thus less contacts. We have found three types of structures that allow for the addition of  $> 3m$  contacts: (i)  $m$  octahedra, where each pair of octahedra share one edge (as in fig 21c), (ii) an open square face created by half an octahedra (as shown in blue in fig 21a), and (iii) the concave  $m$  point face created by octahedra sharing 3 edges (as shown in blue in fig 21d,e). 4 point concave faces are shown, for example, in fig 21e; 5 point concave faces

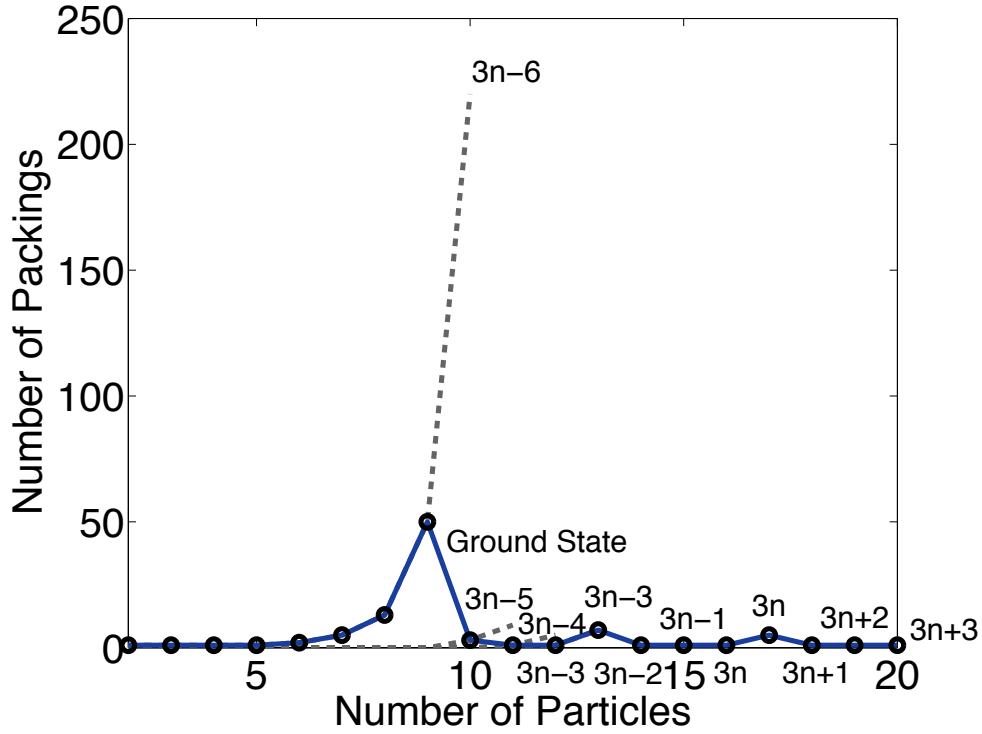


FIGURE 20. Number of packings versus  $n$ , for  $3n - m$  contacts, where  $-3 \leq m \leq 6$ . The ground state degeneracy as a function of  $n$  is shown by the solid curve. Degeneracy for  $n \geq 11$  is conjectured. Dashed curves are shown for  $m = 6, 5, 4, 3$  before and after  $3n - m$  becomes the ground state number of contacts, illustrating the exponential growth of these packings that is primarily due to iterative growth and not to the formation of  $3n - m$  seeds.

in fig 21f,g; and 6 point concave faces in fig 21h,i. To each  $m$  point concave face, it is possible to add one particle with  $m$  contacts. All structures leading to maximal contact packings that we have found thus far are related to octahedra, and we conjecture that this will be the case for all  $n$ . (Interestingly all non-rigid packings found thus far are also related to octahedra, in that they contain the open square faces created by half-octahedral structures; they all contain half-octahedra sharing  $\geq 1$  point.).

There are many fewer ways of adding  $> 3m$  contacts to an  $n - m$  sphere packing than there are of adding  $3m$  contacts, thus leading to a relatively small number of ground state packings when a new maximal number of contacts, as a function of  $n$ , is reached. Thus, each time a packing with a greater maximal number of contacts, as a function of  $n$ , is possible, we expect the ground state degeneracy to either decrease or to remain small. When the functional form for the maximal number of contacts remains constant, we expect the ground state degeneracy to grow rapidly, due in large part to the iterative growth of adding a particle with 3 contacts to packings. Fig. 20 for example, shows that for  $n \leq 9$  the ground state degeneracy increases exponentially because all packings have  $3n - 6$  contacts. But at  $n = 10$  this trend changes because packings with  $> 3n - 6$  contacts become possible. At  $n = 13$  and at  $n = 17$ , rapid growth in the ground state degeneracy resumes as the functional form for the maximal number of contacts remains constant, but for all



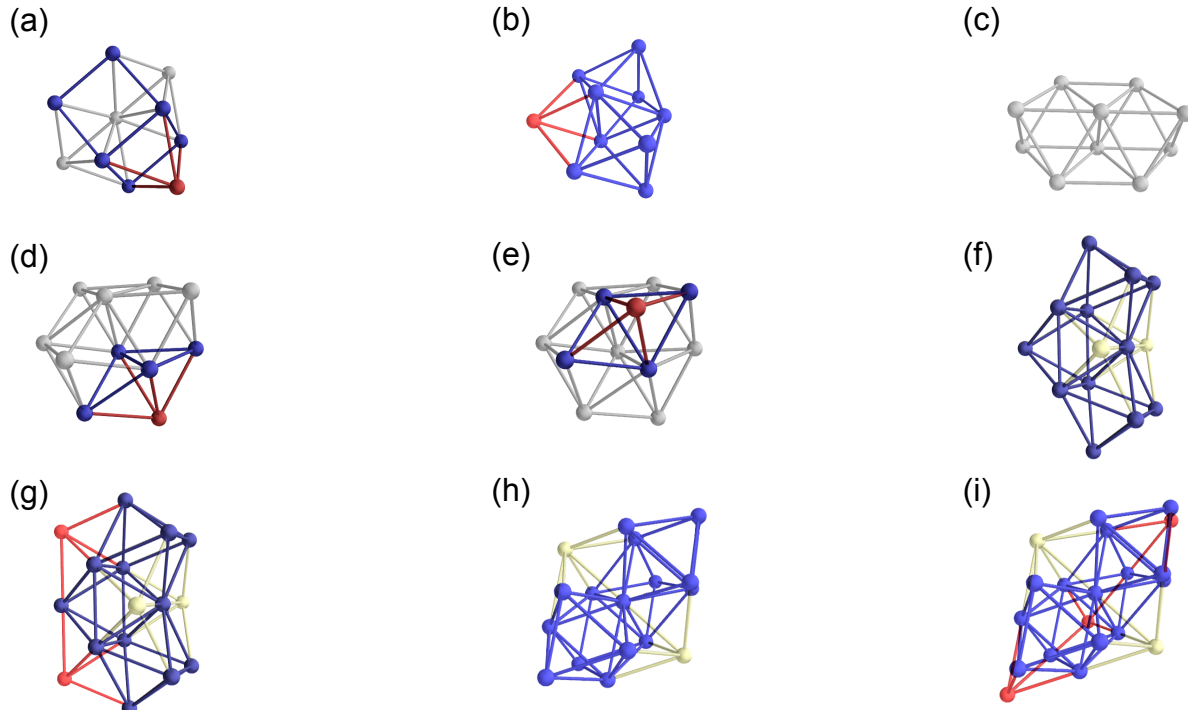


FIGURE 21. Maximal contact packings for  $10 \leq n \leq 20$ . We are reasonably confident that the  $n = 10$  packings shown here correspond to the maximal contact packings, but maximal contact packings of  $n > 10$  are conjectured. (a)-(c) 10 particle packings with  $3n - 5 = 25$  contacts. (a) can be formed either by adding one particle (red) to one of the open square faces (blue) of fig 17a. (b) can be formed by adding one particle (red) to the concave 4 particle face created by 2 joined octahedra (blue). (c) is formed by connecting 2 octahedra by one edge. (d) 11 particle maximal contact packing ( $3n - 4 = 29$  contacts). This can be formed either by adding one particle (red) to the concave 4 particle face created by the 2 joined octahedra of (b), or by adding one particle to the one remaining open square face of (a). (e) 12 particle maximal contact packing ( $3n - 3 = 33$  contacts). This is formed by adding one particle (red) to the concave 4 particle face created by 2 joined octahedra (blue). (f) 14 particle maximal contact packing ( $3n - 2 = 40$  contacts). This is formed by 3 radially connected octahedra (blue) and 2 particles (yellow) added to each of the concave 5 particle faces created by the 3 joined octahedra. (g) 15 and 16 particle maximal contact packings containing  $3n - 1$  and  $3n$  contacts respectively. The 15 particle packing corresponds to the addition of only one of the red particles to the concave 4 particle face of (f), and the 16 particle packing includes both red particles. (h) 17 particle  $3n$  contact packing formed by 4 radially connected octahedra (blue) and 2 particles (yellow) connected to the concave 6 particle faces created by the 4 joined octahedra. At 17 particles,  $3n$  contact packings correspond to this packing as well as packings constructed iteratively from (g). (i) 18,19,20 particle maximal contact packings corresponding to  $3n + 1$ ,  $3n + 2$ , and  $3n + 3$  contacts respectively. Each of these packings is constructed by adding a particle (red) to one of the concave 4 particle faces created by the joined octahedra – the 18 particle packing is constructed by adding one such particle to (h), 19 by adding 2, and 20 by adding 3.

other  $n$ , the ground state degeneracy either decreases or remains constant, because a new maximal number of contacts, as a function of  $n$ , is possible.

At low temperatures, we expect the experimentally observable packings to be dominated by the maximal contact packings. Thus, for  $n = 10$ , and for any  $n$  in which either (i) the maximal number of contacts increases as a function of  $n$  or (ii) the maximal number of contacts does not remain constant for too long ( $\leq 3$  particles), we expect that there are only a small number of packings that will be observable at low temperature. This trend can be seen in the conjectured ground state degeneracy for  $9 < n \leq 20$  in Fig. 20, and we conjecture that a similar low amplitude oscillatory trend might also continue for  $n > 20$ .

**TABLE 5. Number of Contacts Vs Number of Particles.**

The first column corresponds to the number of particles,  $n$ , the 2nd column to the number of contacts that the ground state packing(s) have, and the 3rd column to the number of packings in the ground state. Note that for  $n \geq 11$  these are putative results and thus the number of packings with  $3n - m$  contacts represents a lower bound, and the ground state number of contacts is conjectured (we have not encountered packings with more contacts, but we have not proved that they don't exist).

$n$	Contacts	Ground State Packings
2	$3n - 6$	1
3	$3n - 6$	1
4	$3n - 6$	1
5	$3n - 6$	1
6	$3n - 6$	2
7	$3n - 6$	5
8	$3n - 6$	13
9	$3n - 6$	50
10	$3n - 5$	3
11	$3n - 4$	1
12	$3n - 3$	1
13	$3n - 3$	7
14	$3n - 2$	1
15	$3n - 1$	1
16	$3n$	1
17	$3n$	8
18	$3n + 1$	1
19	$3n + 2$	1
20	$3n + 3$	1

**6.6. Lattice Structure.** The non-rigid new seeds at  $n = 9$  and  $n = 10$ , as well as the maximal contact packings of  $n < 13$  are all subunits of the hexagonally close-packed (HCP) lattice, being combinations of face-sharing tetrahedra and octahedra. Additionally, the structure shown in Fig. 21c is a subunit of either the HCP or face-centered cubic (FCC) lattice. The non-rigid packings are entropically favored, and we thus expect these to form with higher probability at higher

temperatures; while the maximal contact packings are energetically favored, corresponding to the structures that will form with higher probability as the temperature,  $T \rightarrow 0$ . For  $14 \leq n \leq 20$ , the maximal contact packings are not HCP subunits (Fig. 21 f-i).

Frank predicted [18] that icosahedral short-range order would be a hallmark of liquid structure, and experimental studies have shown local cluster-like order in bulk atomic liquids and glasses [38, 42]. And results from a recent study suggest that structural arrest in condensed phases may be related to geometrical constraints at the scale of a few particles [40]. However, the propensity for icosahedra [24, 16] in longer-range systems is absent in ours. We have proven that the icosahedron is *not* the ground state at  $n = 12$ , nor is an icosahedron with a central sphere the ground state at  $n = 13$ . A 12-sphere icosahedron has only  $3n - 6 = 30$  contacts, and in a 13-sphere icosahedron the outer spheres would not be close enough to interact with each other.

It is possible, and perhaps even likely, that the lattice structures corresponding to ground state packings will be periodic with  $n$ . For example, although the ground states for  $14 \leq n \leq 20$  are not commensurate with HCP, the ground states for a finite range of higher  $n$  may be, and may then subsequently return to the lattice structure commensurate with  $14 \leq n \leq 20$ . Detailing the structures of ground state packings for all  $n$ , and geometrical patterns contained therein, is a subject of future work. Furthermore, the appearance of crystalline order, such as HCP, at very low  $n$  may influence nucleation.

## 7. EXTENSIONS AND CONJECTURES

**7.1. The major roadblock for reaching higher  $n$ .** The main roadblock to the *analytical* enumeration of sphere packings at higher  $n$  in the current work is deriving one analytical geometrical rule that can solve for all new seeds. In the next section, we outline a numerical method, based on the triangular bipyramid rule, that is capable of finding *all* solutions of  $\mathcal{A} \rightarrow \mathcal{D}$ , and which can thus solve for all new seeds. However, the implementation of either this numerical scheme or the derivation of an analytical rule would only allow us to enumerate packings of up to about  $n = 14$  spheres. This is because the real limitation of the current method arises from the enumeration of minimally rigid, non-isomorphic adjacency matrices. For  $n < 10$ , the enumeration of such adjacency matrices using *nauty* [36] takes on the order of seconds. For  $n = 10, 11$ , this enumeration takes minutes. For  $n = 12$ , enumerating all minimally rigid, non-isomorphic  $\mathcal{A}$ 's takes approximately 2 hours. Extrapolating, we expect the enumeration at  $n = 13, 14$  to take on the order of 2 days and 2 weeks, respectively. Thus, around  $n = 14$ , we begin to reach the computational limitations of this method, which is due to the enumeration of  $\mathcal{A}$ 's.

Only a very small fraction of adjacency matrices correspond to sphere packings; for example, at  $n = 10$ , out of the 750,226  $\mathcal{A}$ 's, only 223 correspond to sphere packings. Thus, the enumeration of all  $\mathcal{A}$ 's really is a brute force and wasteful step. Further advances in enumerating sphere packings will require overcoming this roadblock. In section 7.3, we propose one method that might be able to overcome this limitation.

**7.2. Applying the Triangular Bipyramid Rule to New Seeds.** The Triangular Bipyramid rule solves for iterative structures but does not work for noniterative ones, which we also showed increase rapidly starting at  $n = 10$ . Here, we discuss how the triangular bipyramid rule might also be applied to new seeds. In this case, the equations for the unknown interparticle distances,  $r_{ij}$ , are implicit and thus must be solved numerically.

Let us consider a general triangular bipyramid, where all 10 distances are potentially unknown (Fig. 22). For  $m$  unknown  $r_{ij}$ , we can construct  $m$  general triangular bipyramids to solve for them (see Fig. 23, for example). Each distance within the triangular bipyramid has a location,

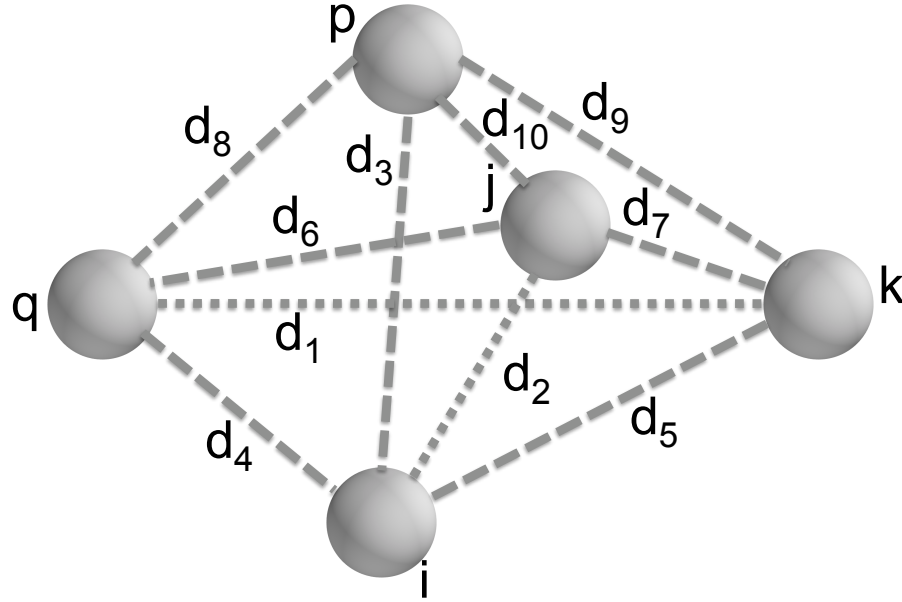


FIGURE 22. **General Triangular Bipyramid.** A triangular bipyramid where all distances, labeled  $d_1 - d_{10}$ , are potentially unknown. The particles,  $i, j, k, p, q$  correspond to the same labeling as in figures 13 and 14. This triangular bipyramid, along with the properties of its ‘3 sub-tetrahedra’ (fig 13), is used to derive the general equation for an unknown relative distance  $r_{ij}$  (appendix A).

$d_i$ . Out of these locations, explicit formulas can always be obtained for  $d_2$  and  $d_3$ . Thus, out of the  $m$  triangular bipyramids, place each unknown  $r_{ij}$  in either  $d_2$  or  $d_3$  at least once. Since new seeds are inherently global structures, be sure that the  $m$  triangular bipyramids contain all  $n$  points amongst them. Also, to avoid redundancy, each triangular bipyramid must contain a unique combination of 5 particles.

We derive the equations for the  $r_{ij}$ , in location  $d_i$ , directly from

$$A_1 = \begin{cases} A_2 + A_3 \\ A_2 - A_3 \end{cases}$$

Writing  $A_1$  as either the sum or product of  $A_2$  or  $A_3$  and solving for  $d_2$  thus yields 2 possible solutions for  $d_2$  (see supplemental information [8] for formula).

For each set of  $r_{ij}$  that is to be solved, construct initial guesses between the bounds of the triangle inequality and no-overlap constraint, and iterate the initial guess with a step size  $\leq$  the minimum difference between different solutions (for rigid structures). There will always exist unknown  $r_{ij} \leq 2R$  because each particle has  $\geq 3$  contacts<sup>18</sup>. These are the  $r_{ij}$  for which there exists a  $k$  satisfying  $\mathcal{A}_{ik} = \mathcal{A}_{jk} = 1$ ,  $\mathcal{A}_{ij} = 0$ . Thus, first solve the set of  $R \leq r_{ij} \leq 2R$ . If unknown  $r_{ij}$  remain, then solve the set of  $r_{ij}$  that now have known triangle inequality bounds, due to the previously solved set of  $r_{ij}$ , repeat until all  $r_{ij}$  have been solved<sup>19</sup>.

<sup>18</sup>This also holds true when each particle has  $\geq 2$  contacts.

<sup>19</sup>We have tested this method on the new seed  $\mathcal{A}$ 's for  $n \leq 8$ , and have shown that it works; however, we have not implemented it for up to  $n = 14$ .

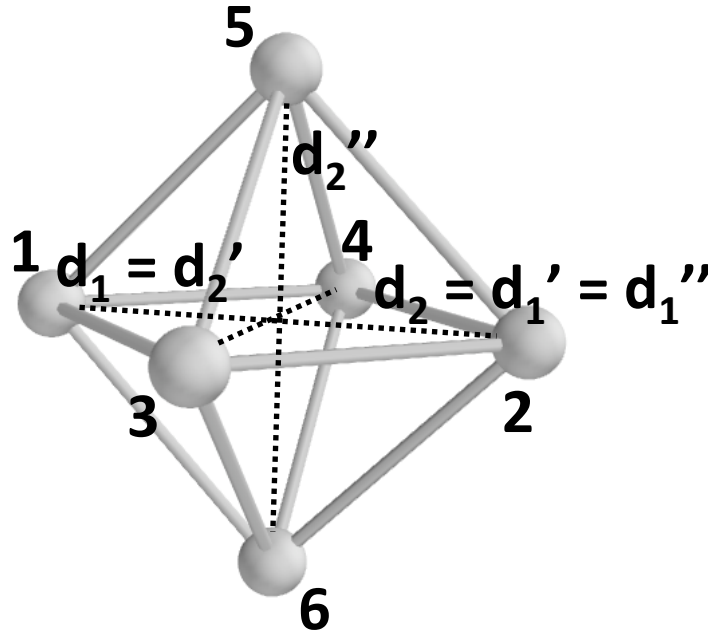


FIGURE 23. **A New Seed and the General Triangular Bipyramid.**

Here we show an example of how to apply the general triangular bipyramid to a new seed in order to solve its unknown distances. This new seed corresponds to the 6 particle octahedron. It has 3 unknown distances,  $r_{12}$ ,  $r_{34}$ , and  $r_{56}$  (dashed black lines). The first triangular bipyramid constructed consists of particles 1, 2, 3, 4, 5, and has unknown distances  $d_1$  and  $d_2$ , corresponding to  $r_{34}$  and  $r_{12}$ , respectively. Note that ( $d_3$  to  $d_{10} = R$ ). The second triangular bipyramid consists of particles 1, 2, 3, 4, 6 and has unknown distances  $d_1'$ ,  $d_2'$  corresponding to  $r_{12}$ ,  $r_{34}$ , respectively. The third triangular bipyramid consists of particles 1, 2, 4, 5, 6 and has unknown distances  $d_1''$ ,  $d_2''$  corresponding to  $r_{12}$ ,  $r_{56}$ , respectively. Note that the first two triangular bipyramids comprise 2 equations and 2 unknowns, and thus are alone sufficient to solve  $r_{12}$  and  $r_{34}$ . Once these 2 distances are known, applying the third triangular bipyramid involves only 1 unknown distance,  $r_{56}$ , and thus follows as applying the triangular bipyramid to an iterative packing.

**7.3. The Bond Breakage Conjecture.** A packing of  $n$  spheres can be formed by (i) taking an  $n - m$  sphere packing, breaking a contact (or bond), adding  $m$  new spheres, and forming the appropriate contacts to complete the packing, or by (ii) breaking one bond of an  $n$  sphere packing and reforming another. From this property, we propose the following theory.

*Bond Breakage Conjecture:* All packings of  $n$  spheres can be obtained by breaking one bond and reforming another in every possible way. For any packing, there exists an  $m$  step path, of

breaking one contact and reforming another, that will form that packing out of another packing with  $3n - 6$  contacts. Each of the  $m$  steps will correspond to an  $n$  particle packing. The end points of the path (i.e. which  $3n - 6$  packing one begins with and which packing one ends up with) determine what value  $m$  takes. For every packing, there exists  $\geq 1$  other packing for which  $m = 1$ .

This suggests an alternative method for enumerating all packings of  $n$  spheres: construct just one  $3n - 6$  contact packing of  $n$  particles (this can easily be done, simply construct a polytetrahedron for example), and then break and reform bonds in all possible ways. For each packing, it is important to explore every combination of breaking and reforming a bond – i.e. to go down all paths, and not just one path.

We have confirmed this conjecture up to as high as we have enumerated packings ( $n = 10$ ) using the following algorithm:

For every  $\mathcal{A}$  that corresponds to a packing

1. For each 1 that appears in the  $\mathcal{A}$ :
  - (a) Swap the 1 with an existing 0. Do this in every possible non-isomorphic way. (This is the mathematical analogue of physically breaking an existing bond and reforming a different bond that was not present in that packing).

For each new  $\mathcal{A}$  that is generated by swapping a 1 and a 0 (these are 1 bond away  $\mathcal{A}$ 's, i.e. where  $m = 1$ ),

- (i) Test for an isomorphism with the  $\mathcal{A}$ 's of all other packings (i.e. all  $\mathcal{A}$ 's other than the one being examined).
- (ii) If an isomorphism is found, stop the examination of this  $\mathcal{A}$ , as it has been shown that there exists a 1 bond bath between the packing being examined and another packing<sup>20</sup>.

Thus implementing this algorithm computationally, we have proven that, for each  $n \leq 10$ , every packing is a 1 bond distance away from  $\geq 1$  other packing of the same  $n$ . We have not proven this for  $n > 10$ , as we have not enumerated all packings of  $n > 10$ , but we suspect that this conjecture holds for all  $n$ .

Mapping out all possible 1 bond distances might be able to shed insight into the kinetic pathways of packings.

To implement the bond breakage conjecture into an improved method for enumerating sphere packings, the bonds must be broken and reformed intelligently, such that unphysical conformations are not explored. If all physical *and unphysical* conformations were to be explored, then we would simply return to the same computational problem we had with enumerating all non-isomorphic  $\mathcal{A}$ 's. One should be able to break a bond and reform it only as is physically possible by calculating the 1 degree of freedom motion that is left over from the one broken bond. Furthermore, one can take advantage of symmetry to, a priori, not explore redundant (i.e. isomorphic) pathways of breaking and reforming bonds.

**7.4. Extensions to Other Dimensions.** The method presented here is, in large part, not dimension specific. The only step which is dimension specific is the set of geometrical rules used to solve  $\mathcal{A}$  for  $\mathcal{D}$ . However, at least for the triangular bipyramid rule (which solves for most of the packings), the geometrical rules can easily be modified to account for a different number of

---

<sup>20</sup>If one is interested in examining all 1 bond paths that exist between all packings, then this same algorithm can be executed without this termination step to yield all possible 1 bond paths.

dimensions,  $d$ . Once this is done, the same method can be used to solve for sphere packings of  $d \neq 3$  dimensions.

**7.5. ‘Lower Dimensional Packings’.** While a packing of  $n$  spheres depends on the dimensionality of its embedding space, there exists a cutoff number,  $m$ , for which the packing of  $n$  spheres remains constant  $\forall d + i$  dimensions,  $i \geq 1$ . For this  $m$ , the  $n$  spheres have accessed all dimensions possible to them, and so the embedding space becomes irrelevant. For example,  $\forall d$ , the unique packing of 1 and 2 spheres is the singlet and doublet, respectively. For 3 spheres, the unique packing in 1 dimension is a linear connected chain of 3 spheres; whereas in 2 dimensions it is the equilateral triangle. For  $d \geq 2$  however, the unique packing of 3 spheres remains the same, it is always the triangle. For 4 spheres, the unique packing in 2 dimensions is the di-triangle; whereas, in 3 dimensions it is the tetrahedron. How does the packing of 4 spheres scale for  $d \geq 3$ ? Does it remain the same? Is it generally true that packings of  $d + 1$  particles remain the same for  $\geq d$  dimensions?

**7.6. Patterns in Adjacencies and Distances.** Does there exist a signature pattern in the  $\mathcal{A}$ ’s or  $\mathcal{D}$ ’s that signifies a packing? In other words, is there a pattern in the distribution of adjacencies (i.e. number of contacts per particle and connections therein) and/or the distribution of distances that corresponds to packings? If such a pattern does exist, it could illuminate a more general method for solving for packings. It also might shed light on the spectrum of allowed solutions for the system of quadratic equations corresponding to the adjacency matrices – detailing which do and do not have real valued solutions in  $\mathbb{R}^3$  satisfying  $\mathcal{D} \geq R$ .

### 7.7. Related Mathematical Problems.

**7.7.1. Erdos Unit Distance Problem.** The Erdos unit distance problem (a.k.a. Erdos Repeated Distance Problem)<sup>21</sup> was posed in 1946 by the Hungarian mathematician, Paul Erdos. It asks what the maximum number of unit (or repeated) distances that can connect  $n$  points in  $d$  dimensions is [17, 9]. This problem is still unsolved. Even in 2 and 3 dimensions, only loose upper and lower bounds are known [14]. The solution to this problem in 3 dimensions, where the unit distance is also the minimum distance, would answer what the maximum number of contacts in any sphere packing is; thus giving the number of contacts corresponding to the ground state packing(s).

**7.7.2. 3 Dimensional Rigidity.** In solving adjacency matrices for both rigid and non-rigid packings that satisfy minimal rigidity constraints in 3 dimensions, this problem is directly related to determining whether a graph is rigid in 3 dimensions. Much work has been done in this field [39, 13, 29, 12, 27, 19], as well as in other dimensions [34]. The existing work on rigidity may help to further inform sphere packings, and the work presented here may in addition be applicable to rigidity theory. In particular, it may allow for the development of a simple method for reading off whether a 3 dimensional graph is rigid or not. By the method presented here, a graph is determined to be non-rigid if  $\exists$  a continuum of solutions to  $\mathcal{A}$ . However, if we can determine a signature pattern that corresponds to all non-rigid (but minimally rigid)  $\mathcal{A}$ ’s, this would allow for a very simple determination of whether a 3D graph is rigid.

---

<sup>21</sup>Without loss of generality, a *repeated distance* can be called a *unit distance*, because one can always uniformly rescale all distances such that the repeated distance is the unit distance. Put another way, ‘a unit’ can be given any value – here, the unit is simply given the value of the repeated distance.

*7.7.3. Solutions to Systems of Polynomial Equations.* The method presented here is inherently solving a system of quadratic equations. Thus presenting an alternative analytical solution to this class of problems. Current standards in the field for analytically solving systems of polynomial equations include Grobner bases [11]; however, these are time-consuming and thus do not scale efficiently with the number of equations. The method presented here solves a certain class of polynomial equations efficiently for a relatively large number of equations. Is it possible to extend this method in order to more efficiently solve large systems of polynomial equations?

*7.7.4. Euclidean Distance Matrix Completion Problems.* Given a symmetric matrix,  $M$ , where only certain elements are specified, the Euclidean distance matrix completion problem is to find the unspecified elements of  $M$  that make  $M$  a Euclidean distance matrix. Euclidean distance matrix and positive semidefinite matrix completion problems are closely linked [30, 31, 32, 33, 26, 4]. In solving adjacency matrices for distance matrices, the method presented here is directly related and potentially directly applicable to the euclidean distance matrix completion problem and, by extension, to the positive semidefinite matrix completion problem.

## 8. CONCLUDING REMARKS

In this work, we present an analytical method for deriving all packings of  $n$  spheres. We carry out this derivation for  $n \leq 10$ ; where the set of  $n = 10$  new seeds is preliminary, and all iterative packings of  $n = 10$  spheres and all packings of  $n \leq 9$  spheres are potentially complete, save the numerical round-off error present from implementing this analytical method computationally.

We find many interesting properties from the sphere packings enumerated up to  $n = 10$ , as well as from the conjectured maximal contact packings of  $11 \leq n \leq 20$ . This problem is directly related to the physics of colloidal clusters, and may have applications to glassy systems and the nucleation of crystals. It is also directly related to unsolved problems in mathematics, such as the Erdos unit distance problem. We consider this work to be the first step in directing the self-assembly of spherical colloidal particles, where the set of sphere packings represents all structures that can be self-assembled out of a system of  $n$  colloidal particles. The second step is to derive a mechanism for directing the self-assembly of any one of these sphere packings such that it is the only packing that can form.

We thank John Lee for consultations in coding, and David Roach and Noam Elkies for helpful discussions. We also acknowledge support from the MRSEC program of the National Science Foundation under award number DMR-0820484, the NSF Division of Mathematical Sciences, and DARPA under contract BAA 07-21.



## REFERENCES CITED

- [1] GNU Multiple Precision Arithmetic Library. <http://gmplib.org/>.
- [2] Multiple Precision Floating Point Computations with Correct Rounding. <http://www.mpfr.org/>.
- [3] *Sage mathematical software*, nice package. <http://www.sagemath.org>.
- [4] A. Y. ALFAKIH, A. KHANDANI, AND H. WOLKOWICZ, *Solving euclidean distance matrix completion problems via semidefinite programming*, Comput. Optim. Appl, (1999).
- [5] N. ARKUS, *Theoretical approaches to self-assembly and biology*, Unpublished PhD Thesis, Harvard University, (2009).  
<http://people.seas.harvard.edu/~narkus/assets/Thesis.pdf.zip>
- [6] N. ARKUS, V. N. MANOHARAN, AND M. P. BRENNER, *Directing the self-assembly of spherical colloidal nanoparticles*, to be submitted to Nanoletters.
- [7] N. ARKUS, V. N. MANOHARAN, AND M. P. BRENNER, *Minimal energy clusters of hard spheres with short range attractions*, Physical Review Letters, 103 (2009), p. 118303.
- [8] N. ARKUS, V. N. MANOHARAN, AND M. P. BRENNER, *Supplementary information*, SIAM Review, (2009).
- [9] D. AVIS, P. ERDOS, AND J. PACH, *Repeated distances in space*, Graphs and Combinatorics, 4 (1988), pp. 207–217.
- [10] P. L. BIANCANIELLO, A. J. KIM, AND J. C. CROCKER, *Colloidal interactions and self-assembly using dna hybridization*, Physical Review Letters, 94 (2005). 058302.
- [11] B. BUCHBERGER, *Grobner bases: A short introduction for systems theorists*, Proceedings of EUROCAST, (2001), p. 1923.
- [12] R. CONNELLY, *On generic global rigidity, in applied geometry and discrete mathematics*, DIMACS Ser. Discrete Math. Theoret. Comput. Sci, (1991), pp. 147–155.
- [13] R. CONNELLY, E. D. DEMAINE, AND G. ROTE, *Infinitesimally locked self-touching linkages with applications to locked trees*, in Physical Knots: Knotting, Linking, and Folding of Geometric Objects in 3-space, American Mathematical Society, 2002, pp. 287–311.
- [14] H. T. CROFT, K. J. FALCONER, AND R. K. GUY, *Problem Books in Mathematics: Unsolved Problems in Intuitive Mathematics*, vol. II, Springer-Verlag, 1991.
- [15] A. D. DINSMORE, J. C. CROCKER, AND A. G. YODH, *Self-assembly of colloidal crystals*, Current Opinion in Colloid and Interface Science, 3 (1998), pp. 5–11.
- [16] J. DOYE AND D. WALES, *Structural consequences of the range of the interatomic potential - a menagerie of clusters*, J. Chem. Soc. Faraday Trans., 93 (1997), pp. 4233–4243.
- [17] P. ERDOS, *On sets of distances of  $n$  points*, The American Mathematical Monthly, 77 (1970), pp. 738–740.
- [18] F. C. FRANK, *Supercooling of liquids*, Proc. R. Soc. London, Ser. A, 215 (1952), pp. 43–46.
- [19] S. J. GORTLER, A. D. HEALY, AND D. P. THURSTON, *Characterizing generic global rigidity*, 2007.
- [20] G.-M. GREUEL, G. PFISTER, AND H. SCHÖNEMANN, *SINGULAR 3-1-0 — A computer algebra system for polynomial computations*, (2009). <http://www.singular.uni-kl.de>.
- [21] D. G. GRIER, *From dynamics to devices: Directed self-assembly of colloidal materials*, Mrs Bulletin, 23 (1998), pp. 21–21.

- [22] R. B. GROSSMAN, Point Groups. <http://www.chem.uky.edu/research/grossman/stereo/pointgroups.html>.
- [23] M. R. HOARE AND J. MCINNES, *Statistical mechanics and morphology of very small atomic clusters*, Faraday Disc. Chem. Soc., 61 (1976), pp. 12–24.
- [24] M. R. HOARE AND P. PAL, *Physical cluster mechanics - statistical thermodynamics and nucleation theory for monatomic systems*, Adv. Phys., 24 (1975), pp. 645–678.
- [25] L. HONG, A. CACCIUTO, E. LUIJTEN, AND S. GRANICK, *Clusters of amphiphilic colloidal spheres*, Langmuir, 24 (2008), pp. 621–625.
- [26] H.-X. HUANG, Z.-A. LIANG, AND P. M. PARDALOS, *Some properties for the euclidean distance matrix and positive semidefinite matrix completion problems*, J. of Global Optimization, 25 (2003), pp. 3–21.
- [27] B. JACKSON, T. JORDN, AND B. JACKSON, *Connected rigidity matroids and unique realizations of graphs*, 2003.
- [28] E. LAUGA AND M. P. BRENNER, *Evaporation-driven assembly of colloidal particles*, Phys. Rev. Lett., 93 (2004).
- [29] M. LAURENT, *Cuts, matrix completions and graph rigidity*, Mathematical Programming, 79 (1997), pp. 255–283.
- [30] M. LAURENT, *A connection between positive semidefinite and euclidean distance matrix completion problems*, Linear Algebra and its Applications, 273 (1998), pp. 9–22.
- [31] M. LAURENT, *Polynomial instances of the positive semidefinite and euclidean distance matrix completion problems*, SIAM J. Matrix Anal. Appl, 22 (1998), pp. 22–874.
- [32] M. LAURENT, *Matrix completion problems*, in The Encyclopedia of Optimization, Kluwer, 2001, pp. 221–229.
- [33] M. LAURENT, S. POLJAK, AND F. RENDL, *Connections between semidefinite relaxations of the max-cut and stable set problems*, Mathematical Programming, 77 (1995).
- [34] L. LOVASZ AND Y. YEMINI, *On generic rigidity in the plane*, SIAM J. Algebraic Discrete Methods, (1982), pp. 91–98.
- [35] V. N. MANOHARAN, M. T. ELSESSER, AND D. J. PINE, *Dense packing and symmetry in small clusters of microspheres*, Science, 301 (2003), pp. 483–487.
- [36] B. MCKAY, *Practical graph isomorphism*, Congressus Numerantium, 30 (1981), pp. 45–87.
- [37] G. MENG, N. ARKUS, M. P. BRENNER, AND V. N. MANOHARAN, *The free energy landscape of clusters of attractive hard spheres*, Science, accepted.
- [38] H. REICHERT, O. KLEIN, H. DOSCH, M. DENK, V. HONKLMARI, T. LIPPMANN, AND G. REITER, *Observation of five-fold local symmetry in liquid lead*, Nature, 408 (2000), pp. 839–841.
- [39] T. REPORTS, T. JORDN, B. JACKSON, AND B. JACKSON, *The dress conjectures on rank in the 3-dimensional rigidity matroid*, 2003.
- [40] C. P. ROYALL, S. R. WILLIAMS, T. OHTSUKA, AND H. TANAKA, *Direct observation of a local structural mechanism for dynamic arrest*, Nat. Mater., 7 (2008), pp. 556–561.
- [41] T. W. SHATTUCK, *Rotational constant calculator*, Colby College Chemistry.
- [42] H. W. SHENG, W. K. LUO, F. M. ALAMGIR, J. M. BAI, AND E. MA, *Atomic packing and short-to-medium-range order in metallic glasses*, Nature, 439 (2006), pp. 419–425.
- [43] N. J. A. SLOANE, R. H. HARDIN, T. D. S. DUFF, AND J. H. CONWAY, *Minimal-energy clusters of hard spheres*, Disc. Comp. Geom., 14 (1995), pp. 237–259.
- [44] D. Y. WANG AND H. MOHWALD, *Template-directed colloidal self-assembly - the route to ‘top-down’ nanochemical engineering*, J. Materials Chem., 14 (2004), pp. 459–468.

- [45] G. M. WHITESIDES AND B. GRZYBOWSKI, *Self-assembly at all scales*, Science, 295 (2002), pp. 2418–2421.

SCHOOL OF ENGINEERING AND APPLIED SCIENCES, HARVARD UNIVERSITY, CAMBRIDGE, MA 02138